

The Global Scaling[®] Theory

A short summary

Dipl. Ing. FH Andre Waser*



Issued: August 06, 2001

Last revision: January 07, 2004

This summary paper emerged during my studies of Global Scaling theory. This document bases on publications and lectures made by the inventor of Global Scaling theory – Dr. rer. nat. Hartmut Muller. In this introductory document the basic terms of Global Scaling theory are explained step by step.

This document serves as a base for discussions with others interested in Global Scaling. Comments, amendments or corrections are welcome and some of them will be included in future document updates, if necessary.

* André Waser, Birchli 35, CH-8840 Einsiedeln, www.global-scaling.ch

Global Scaling[®] is a registered trademark of the Institute for Space-Energy-Research GmbH in memoriam Leonard Euler in Wolfratshausen, Germany.

All figures and texts in this document are protected by international copyright laws. It is permitted to produce copies of any kind of this document or parts of it without written permission by AW-Verlag.

This is a translation of the German original document “Eine kurze Einführung in die Global Scaling Theorie” by Andre Waser.

The German version always supersedes this English version.

Content

INTRODUCTION	5
Term „Global Scaling“	5
Logarithmic distribution in nature	6
Gravitation	6
Zero-point field.....	6
Entropic force	7
CREATION OF STRUCTURES IN VACUUM.....	9
The oscillating beads.....	9
Global Scaling continuous fraction.....	12
CONTINUOUS FRACTIONS	13
Notation of continuous fractions	13
Representation of real numbers with continuous fractions	13
Golden Mean ϕ	14
Continuous fractions and quadratic equations	16
Recursion and continuous fractions	16
Convergence of continuous fractions.....	17
Equivalence transformation of continuous fractions	17
THE MULLER FRACTAL	18
Exact Global Scaling continuous fraction	18
Physical dimension.....	18
Calibration unit	18
The logarithmic line.....	19
Denominators.....	19
Nodal points	20
Border area.....	20
Abort criteria of Global Scaling continuous fraction calculations	21
Muller fractal.....	22
Fractal dimension.....	23
Influence of numerator to the Muller fractal.....	24
Working with the Muller fractal.....	24
FIRST PHYSICAL INTERPRETATIONS	25
Standing gravity waves	25
Mass line	26
Graviton flow	27
Compression and decompression (fusion and decay).....	27
Phase on the logarithmic line	29
Super-stability.....	31
Length line	32
Modes on the logarithmic line	32
Frequency line.....	33
Time line.....	34

TIME.....	35
Global time wave	35
Experiments of Shnoll et. al.	36
Kozyrev's concept about the properties of time.....	39
Experiments of Erwin Saxl.....	41
Experiments of Guido Ebner and Guido Schuerch.....	42
Time, energy and entropy.....	43
Local and global time line	44
Fluctuations	45
The role of thermodynamics	45
Prognosis of stochastic processes	46
Reflection of time	46
Near field action and action-at-a-distance.....	46
Energy exchange via nodal points.....	47
Possible energy source: The cosmic background radiation.....	48
Acknowledgement	49
Global Scaling Lectures.....	49
APPENDICES	50
Appendix 1: Continuous fractions of some irrational numbers	50
Appendix 2: Calibration units.....	52
Appendix 3: Values of mass line	53
Appendix 4: Table of some super-stable masses.....	54
Appendix 5: Values of length line	55
Appendix 6: Values of frequency line	56
Figures.....	57
References.....	59
Original publications about Global Scaling in raum&zeit journal.....	61

An analysis of current problems in electrodynamics and gravitation always leads to the conclusion, that basically new concepts or physical models are necessary to describe natural processes more accurate than today. The paradigm in today's physics is well known.

The main demand on a new physical model is to postulate as little premises as possible to explain as much physical phenomena as possible. With a world view of reductionism only, this is not achievable. Hence the author has proposed a concept of a self-reproducible (autopoietic) physics about ten years ago^[43].

Many authors have formulated new and holistic physical models in the last years. Concerning this, the theory of Burkhard Heim^[15] must be noted. Unfortunately his complex work is not written down in an easy understandable form (although for physicists and mathematicians). And also some controversial models as for example the vortex model of Lord Kelvin^[40] (William Thomson) do exist, which are able to explain many structures and properties of matter with a very small set of premises.

The Global Scaling theory (GST) is a holistic theory, capable to explain the cause of many physical phenomena with a very low set of assumptions. This theory is further capable to explain some experimental results, which – due to their scientific impact – are not well accepted. Naturally, also the Global Scaling theory keeps some questions unanswered, but hopefully these might be answered satisfactorily in the near future.

Only a limited number of fragmented and mostly compressed texts about Global Scaling are available today. It's a goal of this document to overcome this restriction and give interested readers a first glimpse about the Global Scaling theory "as a whole".

Term „Global Scaling“

Almost 30 years ago, biologists (Schmidt-Nielsen, Shnoll, Cislenco, Shirmunski and more) recognized that organisms have a much better survival and reproduction chance, if their body size is in a certain value range. Amazingly this is widely independent of their species.

The crucial discovery was made by the Russian-Ukrainian biologist Cislenco^[7]. In 1981 he published the result of his 23 year long data collection: The biological preferred value ranges are arranged in regular steps along a logarithmic scale. Cislenco substantiated this fact for 4727 species of mammals, over 5000 species of critters, 452 species of birds, about 1900 species of amphibians, 381 species of fresh-water fishes, 218 fish species of the North polar sea, over 21.000 species of insects as well as an uncounted number of species of plants, mushrooms and bacteria. Today one speaks in this context of a logarithmic scale invariance of the distribution of biological species according to their body size and masses of organisms.

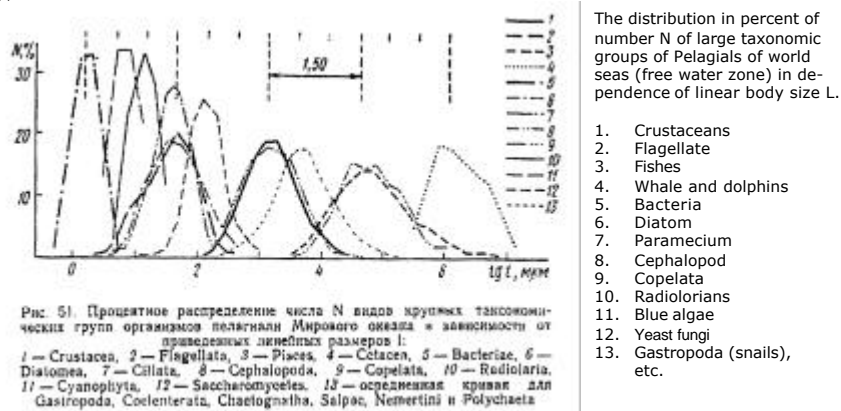


Figure 1: Cislenco [7]: The distribution of species regarding organism mass plotted on a logarithmic scale. The regular distance between the maximums are clear visible.

In about the same time physicists discovered the phenomena of scale invariance (scaling) in distributions of elementary particles in dependence of their rest mass (Bjorken, Feinmann, Muller). 1982 Muller has proved the same scaling effect for all particles, nucleus, atoms as well as asteroids, moons, planets and stars. Scaling is a global phenomena and possibly the blue print of the universe. Hence the term „Global Scaling“ is founded satisfactory.

Logarithmic distribution in nature

A logarithmic distribution in nature is not an exception but a rule^[46]. A natural distribution without at least a partial logarithmic distribution does not exist at all. The reason of this lies basically in exponential (multiplicative) growth processes in nature. A natural distribution can be transformed back to a well-known symmetric Gauss'ian distribution with a logarithmic function only. Therefore, it is not astonishing but explicitly a basic condition, that a logarithmic scale must be included in a holistic physical theory.

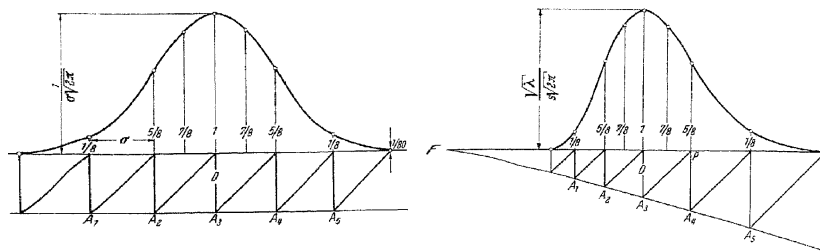


Figure 2: The Gauss'ian regular distribution is expected for additive growth processes whereas the logarithmic distribution arises for multiplicative (natural) growth processes [12].

Gravitation

Gravitation is the weakest natural force we know. Gravity is about 10^{40} times weaker than electric forces. Until the advent of Einstein's general theory of relativity, gravitation has been interpreted in Newtonian theory as a force acting at a distance. This force was thought to be inherent to every mass and has only attractive polarity. Still today the cause of gravity is not known completely. For example, the model of a curved space-time does not answer the question how a mass should be able to bend space and time.

Many researchers have viewed at centripetal oriented gravity as a formative force. The centrifugal and dissipative (destructive) force does exist in coexistence with gravity. For example Walter Russell^[30] or Viktor Schauberger^[31] drawn a world model, where gravity is a constructive (positive) force.

Zero-point field

In Global Scaling theory as well as in other alternative physical theories it is assumed, that the pure empty space (vacuum) does not exist because it is filled somehow by a medium. In earlier theories this medium was modeled as a fluid^[44]. Today the existence of the quantum vacuum containing a zero-point fluctuation is widely accepted (Zero Point Field ZPF)^[29]. According to Harold Puthoff^[28] this modern description of vacuum is capable to generate such basic actions like gravity or inertia.

The vacuum particles are mostly photons. They constitute the all pervading and so called **zero-point field**. The radiation of this field is always measurable in space, even if we would evaporate a certain area in space completely out of material and thermal radiation. Because of this zero-point radiation, electric charges never come to a complete rest but always show some zero-point oscillations.

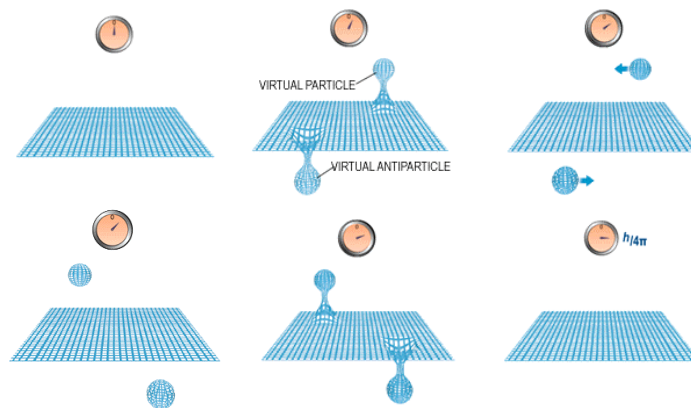


Figure 3: The grid stands for the energetic ground state of space. Spontaneous emission and absorption of particles and anti-particles take place within a very short time. The existence of the particles cannot be proven directly but indirectly via the effects of the resulting zero-point radiation.

Also in Global Scaling theory it is assumed that the vacuum is not empty and a medium does exist. The medium particles are called gravitons and are responsible – beside other things – for the gravity force. They have a very small rest mass, but above zero (more later). Additionally, the gravitons and the photons are the same particles, whereas follows, that according to Puthoff the photons of the zero-point radiation and the gravity particles are equivalent. Accordingly it is clearly expected that gravity and electromagnetism must have common roots.

Entropic force

Also in Global Scaling theory gravity is a constructive or entropic force. As an explanation of the entropic force we refer to a newer experiment carried out by Hans Henning von Grunberg and Clemens Bechinger at the University of Konstanz^[12]. The two physicists placed polystyrene balls with a diameter of some micro-meters onto a water solution, where the balls float on the water and arrange themselves with an evenly distribution, as commonly expected. After inserting the balls, the system is closed and achieves its state of maximum entropy. Now, for a short time the system is opened again and even smaller polystyrene balls with a diameter of about 150 nm are inserted. Then the system will be closed again. But now the distribution of the larger balls change dramatically. They tend to build clusters and move to the jar walls so that the smaller balls have maximum space for movement. Again the entropy for the smaller balls is maximized, but not anymore for the larger balls.

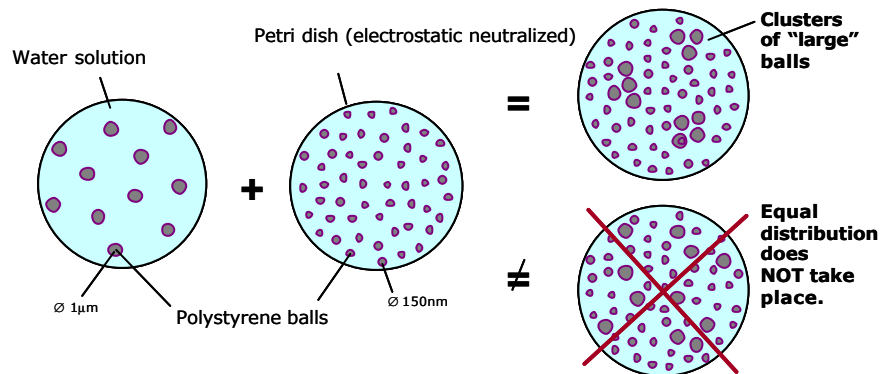


Figure 4: The Experiment of von Grunberg and Bechinger: The „larger“ polystyrene balls in a water solution are pressed together by the „smaller“ polystyrene balls.

But, who tells the larger balls that they must build clusters to enable the smaller balls a maximum of entropy? The authors came to the conclusion that they have found a new force. They named it *entropic force*^[14]. They also succeeded to prove that this new force is neither of electromagnetic nor of gravitation origin.^[2]

The similarity of this new force with the gravity effect is obvious^[25]. Because of the presence of the smaller balls, the larger balls are pressed together. And exactly this mechanism we find in the universe, from smallest up to largest scales. The small balls are equivalent to gravitons or photons and the larger balls are clusters of this smaller balls, which under certain stable circumstances form long living particles, which in turn can be observed as masses of all kind, or as elementary particles, planets or galaxies.

2. Creation of structures in vacuum

First, a space filled with gravitons has no further structures. But as we observe, this is not the case. Therefore, somehow structures have emerged out of the vacuum and build that, what we perceive as matter and what we are able to feel, detect and measure with our equipment. But how this structures are created?

To build a structure it is basically necessary that we have a feedback system, i.e. a system where the output or a part of it is feed back to the input. More information about this can be found in the paper „Autopoietic Systems“^[43]. Accordingly the creation of structures is a growth function, which can end up in three different kind of states – or as the mathematician would say – in three different kind of a **attractors**:

- a) Static; the system tends to a stable final value
- b) Dynamic; the system oscillate between two or more finite values
- c) Chaotic; the system oscillates between infinite values.

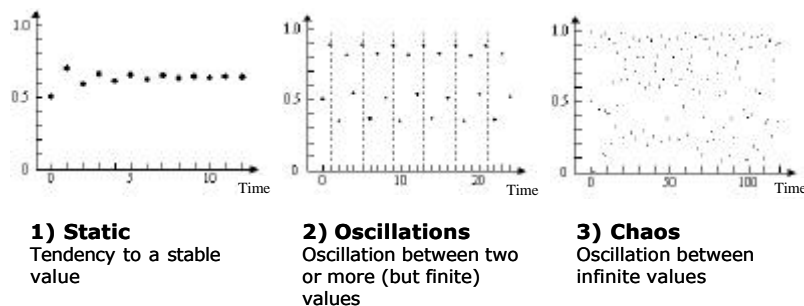


Figure 5: The three basic attractors for a growth function: static – oscillating - chaotic.

The only possible practicable attractor for creating some stable structures is this one in the middle. Oscillations can spread in every medium. Depending on viscosity of the medium – as it would be named in fluid mechanics – these oscillations are damped and will have a finite propagation speed. Now the question arises about the model we should select to describe, how an oscillating medium is able to create structures out of the vacuum.

The oscillating beads

Global Scaling theory answers this crucial question with the model of oscillating beads. The model of oscillating beads is much accurate than the model of an oscillating string, but on a closer look also a string will become a beads. Important is the statement, that the beads can have different masses and distance to the next bead. Also this is the case for a string which finally is composed of atoms only.

To enable the propagation of an oscillation it is also required that a string or beads is of finite length, is clamped somewhere and it must be supplied with energy all the time to cover it's damping losses.

The problem of an oscillating string has been solved in physics for the very special case of a homogenous, isotropic und continuous (not granular) string, whereas the oscillation itself must follow an analytic function (no gaps and continuous). The corresponding partial differential equation and its solution is known from Rond d'Alembert^[1] since 1747 and is written for one single space dimension as

$$\frac{\partial^2 y(x,t)}{\partial x^2} = \frac{\partial^2 y(x,t)}{\partial t^2} \quad (1)$$

with the general solution

$$y(x,t) = f(x+t) + g(x-t) \quad (2)$$

A year later, the Swiss mathematician Leonard Euler^[2] has presented a slightly different equation with

$$\frac{\partial^2 y(x,t)}{\partial x^2} = \frac{1}{c^2} \frac{\partial^2 y(x,t)}{\partial t^2} \quad (3)$$

with the general solution

$$y(x,t) = f(x+ct) + g(x-ct) \quad (4)$$

Euler was interested to find also a solution to the problem of oscillating strings, whereas the initial condition $y(x, t)$ is not continuous as it's the case when a string is plucked with a hard object. But only in 1807 Joseph Fourier has „solved“ the problem with his famous Fourier analysis of an infinite sum of analytical sine and cosine functions^[48].

In a close look the reader might have recognized, that such a Fourier analysis is an endless sum of sine and cosine functions, which must be taken simultaneously at the same time, does not really fulfill the requirement of natural laws. But how nature should be able to calculate an infinite sum simultaneously?

If we look at natural objects, we recognize that they are granular, i.e. they consist of objects of a finite size. Therefore analytical mathematic functions are always approximations only. Now, let's look at a beads instead of a string. First each single bead shall have equal mass and all are connected with mass-less threads of the same length, which fulfill Hook's law. The possible eigenvalues (resonance frequencies) N of the beads increase proportional to the number of beads N . The oscillation with highest possible frequency will have a pure triangle shape and each bead is located at its maximum displacement position. The beads will not have higher resonance frequencies. Accordingly each beads has a finite number of resonance frequencies. This was not the case for a theoretic continuous string.

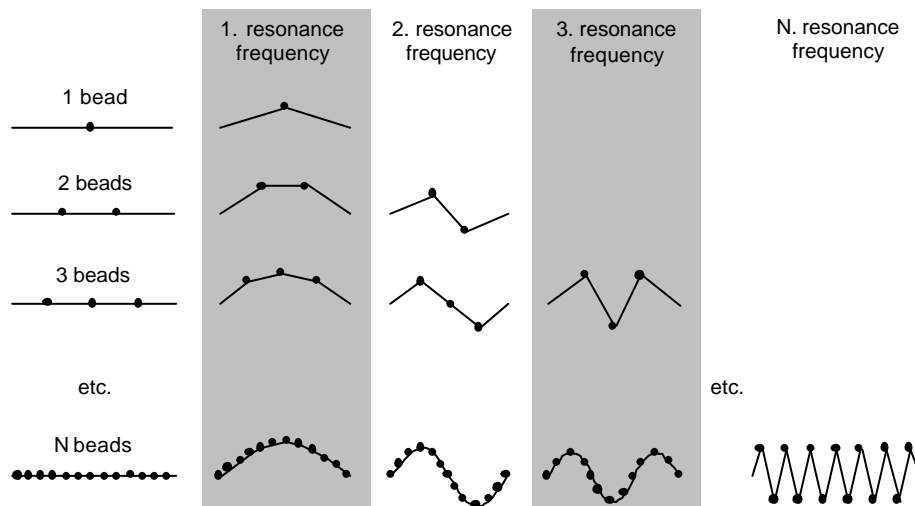


Figure 6: A beads with 1, 2, 3, ..., N beads of same mass have a corresponding number of possible transversal resonance frequencies.

Now, in general a beads does not have beads with equal mass and separation distance but all values can be arbitrary. Such a complex problem of a general oscillation beads has been solved in two steps. Two centuries ago T. J. Stieltjes^[39] searched in a first step the solution for the problem of mass distribution on a straight line and he found a general solution in the form of continuous fraction equations. This paper gives the solution for the static case where the momentum of a line of masses is balanced, but the dynamic case of oscillation was still unsolved.

Then in the year 1960 F. R. Gantmacher and M. G. Krein^[11] worked on the problem of small oscillations in mechanical systems and they published in appendix II a very important result „About a remarkable problem for beads and about Steltjes continuous fractions“. In this appendix they generalized Steltjes continuous fractions for dynamical systems and found some physical interpretation of the results.

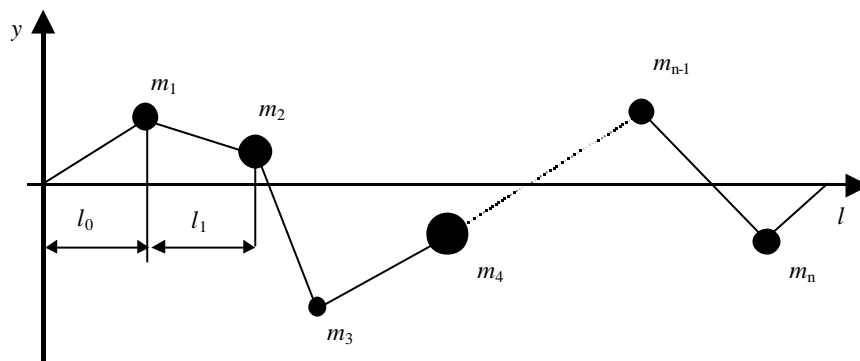


Figure 7: The general oscillating beads

To solve the problem of the oscillating beads Gantmacher and Krein have intersected the beads in small „quanta“. Each quanta corresponds with a line section l_i ($i=0, 1, \dots, n$) from one bead of mass m_i ($i=1, 2, \dots, n$) to the next bead. Each such quanta still follows the Lagrange equation. With a recursion process of the oscillations of all this quanta finally the total oscillation of the whole beads is the result. This quantization und recursive algorithms are used today in many computer simulations.

Gantmacher and Krein found all resonance frequencies ω of a beads with a continuous fraction like:

$$\frac{y_{i+1}l_i}{y_{i+1} - y_i} = l_i/\sigma + \frac{1}{-m_i\omega^2 + \frac{1}{l_{i-1}/\sigma + \frac{1}{-m_{i-1}\omega^2 + \frac{1}{\ddots + \frac{1}{l_1/\sigma + \frac{1}{-m_1\omega^2 + \frac{1}{l_0/\sigma}}}}}} \quad (5)$$

where y_i and y_{i+1} denotes the position of the two threads' ends, l_i the different intersections between the beads with mass m_i . Then ω is the resonance frequency of the whole beads and σ is the tension in the thread. Finally the solution for this complex problem becomes unexpectedly simple. The central element of this solution is of course the continuous fraction.

Global Scaling continuous fraction

To explain the creation of structures out of the graviton media Muller^[23] starts with this Gantmacher-Krein continuous fraction and develops the Global Scaling continuous fraction with the aid of Euler's transformation and with $\sigma = 1, -\omega^2 = 1/e$, where the Euler number e is the base of natural logarithm. He found the result in the form

$$\ln\left(\frac{X}{Y}\right) = N_0 + \frac{e}{N_1 + \frac{e}{N_2 + \frac{e}{\ddots N_{L-1} + \frac{e}{N_L}}}} \quad (6)$$

This finite continuous fraction has the length L . The result (or the synthesis) of this continuous fraction is set equal to the natural logarithm of the quotient of X and Y . X stands for an arbitrary physical quantity or dimension. Y denotes the calibration unit to calibrate the physical dimension X . This is necessary to make the logarithm argument free of units.

To calibrate a physical dimension X it is principally possible to use every desired value for Y . But it would make sense to use only such values that are very stable in nature. Therefore, in Global Scaling such a calibration unit is called super-stable. The most stable and long living elements known are the electron and the proton. As Muller^[18] has shown, it's of high advantage to use the proton rest mass as the natural calibration unit. More about the different calibration units you find in appendix 2.

3. Continuous fractions

Before we start examining the specialties of this Global Scaling continuous fraction some general information about continuous fractions shall be given in this chapter. Readers who are familiar with this can proceed directly to the next chapter.

Notation of continuous fractions

Elementary continuous fractions have the form

$$b_0 + \frac{a_1}{b_1 + \frac{a_2}{b_2 + \frac{a_3}{\ddots \frac{a_{n-1}}{b_{n-1} + \frac{a_n}{b_n}}}}} \quad (7)$$

Also shorthand notations are known as

$$b_0 + a_1 / (b_1 + a_2 / (b_2 + a_3 / (b_3 + \dots + a_n / b_n))) \quad (8)$$

or

$$b_0 + \frac{a_1}{|b_1|} + \frac{a_2}{|b_2|} + \frac{a_3}{|b_3|} + \dots + \frac{a_n}{|b_n|} \quad (9)$$

or

$$b_0 + \frac{a_1}{b_1} + \frac{a_2}{b_2} + \frac{a_3}{b_3} + \dots + \frac{a_n}{b_n} \quad (10)$$

The numerator a_i of a continuous fraction is called **partial numerator**, the denominator b_i **partial denominator** accordingly, except the first term b_0 , which often is called as **free member**. These terms are also used in Global Scaling. If all denominators are equal to one ($a_i = 1$), it is possible to write a continuous fraction very short as

$$[b_0; b_1, b_2, \dots, b_n]. \quad (11)$$

Continuous fractions with all denominators equal to 1 are called **regular or simple continued fractions**. And if the denominators are different from 1 but all are equal and constant ($a_i = a = \text{constant}$), also a very useful notation exists as

$$a [b_0; b_1, b_2, \dots, b_n]. \quad (12)$$

Representation of real numbers with continuous fractions

A continuous fraction always contains positive or negative natural numbers without the number zero. For simple or regular continuous fractions the following facts are known:

1. Each infinite continuous fraction is convergent and represents a real number.
2. Each real number can be decomposed in a continuous fraction. The result is unique.
3. For each positive real number a unique regular continuous fraction does exist.

Additionally for all un-branched continuous fractions it is:

4. If a continuous fraction is of finite size, the result will be a rational number (a rational number can be written as a quotient of two natural numbers).
5. If a continuous fraction is of infinite length, the result will be an irrational number.
For irrational numbers no quotient of two natural numbers exists (example: π).

Therefore each real number can be represented by an un-branched continuous fraction. In appendix 1 you find some examples of continuous fractions of irrational numbers. The periodic infinite continuous fractions, as for example the square root of three

$$\sqrt{3} = 1.7320508 \dots = [1; 1, 2, 1, 2, 1, 2, 1, 2, 1, \dots] = [1; \overline{1, 2}]$$

delivers so called quadratic irrational numbers. The result of non-periodic continuous fractions will be a transcendent number as π or e .

By using a decimal representation of a number, it's most of the time not possible to decide if it's a rational, irrational or even transcendent number within a short time. But just with the length of a continuous fraction, this question can be answered always very quickly.

Golden Mean f

Many books about the golden mean are known^[2]. Here we take a look about the connection to continuous fractions only. The golden mean is a solution of the quadratic equation

$$x^2 - x - 1 = 0 \tag{13}$$

The solutions are

$$x = \frac{1}{2} \pm \sqrt{\frac{1}{4} + 1} = \frac{1}{2} (1 \pm \sqrt{5}) \Rightarrow x_1 = \frac{1 + \sqrt{5}}{2}, \quad x_2 = \frac{1 - \sqrt{5}}{2} = x_1 - 2 \tag{14}$$

The golden mean is equal to the solution $x_1 = 1.618033\dots$. The quadratic equation can be transformed to

$$x^2 - x - 1 = 0 \rightarrow x^2 = x + 1 \rightarrow x = 1 + \frac{1}{x} \tag{15}$$

Now, by repeatedly replacing x in the left side of equity sign, slowly an infinite continuous fraction will develop:

$$x = 1 + \frac{1}{x} \rightarrow 1 + \frac{1}{1 + \frac{1}{x}} \rightarrow 1 + \frac{1}{1 + \frac{1}{1 + \frac{1}{x}}} \rightarrow \dots \rightarrow 1 + \frac{1}{1 + \frac{1}{1 + \frac{1}{1 + \frac{1}{\dots}}}} \tag{16}$$

This continuous fraction represents the solution x_1 of the quadratic equation (13). The other solution x_2 is found by a similar transformation of (13) as

$$x^2 - x - 1 = 0 \rightarrow x(x - 1) = 1 \rightarrow x = -\frac{1}{1 - x} \tag{17}$$

whereas the continuous fraction for the second solution x_2 follows as

$$x = -\frac{1}{1 - x} \rightarrow -\frac{1}{1 + \frac{1}{1 - x}} \rightarrow -\frac{1}{1 + \frac{1}{1 + \frac{1}{1 - x}}} \rightarrow \dots \rightarrow -\frac{1}{1 + \frac{1}{1 + \frac{1}{1 + \frac{1}{\dots}}}} \tag{18}$$

The golden mean can also be represented in the form of equation (15) and is

$$\phi^2 - \phi - 1 = 0 \rightarrow \phi = 1 + \frac{1}{\phi} \quad (19)$$

Now let's have a look at the approximate fraction to the infinite continuous fraction (16). These are

$$\frac{1}{1} = 0, \quad \frac{1}{1+1} = \frac{1}{2}, \quad \frac{1}{1+\frac{1}{2}} = \frac{2}{3}, \quad \frac{1}{1+\frac{2}{3}} = \frac{3}{5}, \dots, \frac{F_n}{F_{n+1}} \quad (20)$$

where F_n is the Fibonacci number n . A Fibonacci number is found by stepwise development of the number 1 as:

$$\begin{aligned} F_1 &= 1 \\ F_2 &= F_1 + 1 = 2 \\ F_3 &= F_2 + F_1 = 3 \\ F_4 &= F_3 + F_2 = 5 \\ F_5 &= F_4 + F_3 = 8 \\ &\dots \\ F_n &= F_{n-1} + F_{n-2} \end{aligned} \quad (21)$$

This kind of stepwise calculation by using the results of a previous calculation is called a **recursion**. If n is chosen „high enough“, the result of equation (20) will be the golden mean ϕ again. Accordingly it is possible to compute the golden mean with a continuous fraction or with a recursion process:

$$\begin{aligned} [1] &= F_1/F_1 = 1 \\ [1;1] &= F_2/F_1 = 2 \\ [1;1,1] &= F_3/F_2 = 3/2 = 1.5 \\ [1;1,1,1] &= F_4/F_3 = 5/3 = 1.\overline{6666} \\ [1;1,1,1,1] &= F_5/F_4 = 8/5 = 1.60 \\ [1;1,1,1,1,1] &= F_6/F_5 = 13/8 = 1.625 \\ [1;1,1,1,1,1,1] &= F_7/F_6 = 21/13 = 1.615384\dots \\ [1;1,1,1,1,1,1,1] &= F_8/F_7 = 34/21 = 1.619047\dots \\ &\dots \\ [1;1,1,1,1,1,1,\dots,n \cdot 1] &= F_n/F_{n-1} \xrightarrow{n \text{ very large}} 1.618033988\dots = f \end{aligned} \quad (22)$$

This development shows how a continuous fraction can be developed by a recursion process. With each calculation step the result gets more and more accurate. Now we look at equation (16) and we find

$$x_n = \frac{1}{1 + x_{n-1}} \quad (23)$$

In nature the golden mean is build „automatically“ almost everywhere. It's the most basic recursion (growth) process. In Global Scaling all natural structures are granular and are finally composed of gravitons. Therefore the creation of structure is equivalent to the clustering of such gravitons. Or in other words, in nature all mass elements can be represented by a whole natural number. No decimal numbers are required.

In nature no decimal numbers exist. Also the golden mean is not a decimal number as often written in text books. Moreover nature is “only” capable of constructive or destructive growth processes which happens always at least in parts recursively^[43]. The very

basic recursive equation (23) shows clearly the evolution process in nature. Nature „calculates“ – or better approximates – the golden mean step by step according to this very simple rule. And this consumes time. And with every time step the value of ϕ gets more and more accurate.

This conclusion is very important and should not be underestimated. One direct conclusion is, that time somehow must elapse in quanta rather than absolutely continuous. This important conclusion is also supported by Global Scaling, as we will see later in this document.

Continuous fractions and quadratic equations

The special development in equation (16) can be generalized for quadratic equations.

$$x^2 + Bx + C = 0 \rightarrow \begin{aligned} x_1 &= -B - \frac{C}{x_1} \\ x_2 &= \frac{-C}{B + x_2} \end{aligned} \quad (24)$$

where B and C are whole numbers. Thus it follows, that the result of homogenous quadratic equations (24) can be written as infinite continuous fractions always.

On the other side it's always possible to derive a quadratic equation from periodic continuous fractions as the following example shows.

$$x = 2 + \frac{2}{1 + \frac{1}{2 + \frac{1}{1 + \frac{1}{2 + \dots}}}} \rightarrow x = 2 + \frac{2}{1 + \frac{1}{x}} \rightarrow x^2 - 3x - 2 = 0 \quad (25)$$

Recursion and continuous fractions

The recursion process is a basic criteria for generation of continuous fractions, as we have seen with the golden mean (22) example. Instead of using the special case of Fibonacci numbers, a continuous fraction always can be represented as a quotient of two arbitrary number series a_n and b_n :

$$x_n = \frac{a_n}{b_n} \quad (26)$$

These series can represent the recursive description of rational numbers. Now we start with a finite continuous fraction of length k

$$x_k = b_0 + \frac{a_1}{|b_1|} + \frac{a_2}{|b_2|} + \dots + \frac{a_k}{|b_k|}, \quad x_0 = b_0 \quad (27)$$

If a continuous fraction for x will become infinite ($n \rightarrow \infty$), this is also called an **approximate fraction**. With the definitions

$$A_k := b_k A_{k-1} + a_k A_{k-2} \quad A_{-1} := 1 \quad A_0 := b_0 \quad (28)$$

$$B_k := b_k B_{k-1} + a_k B_{k-2} \quad B_{-1} := 0 \quad B_0 := 1 \quad (29)$$

we can represent an approximate fraction with two recursive terms $A_k(a_k, b_k)$ and $B_k(a_k, b_k)$ as

$$x_k = \frac{A_k}{B_k} \quad (30)$$

Feedback processes often result in fractals ^[43].

Convergence of continuous fractions

Similar to infinite mathematical series, again for infinite continuous fractions arises the question, whether x tends to a stable value with an increasing k , or not. If yes, the continuous fraction is convergent.

Equation (30) can be used to define the convergence of continuous fractions: *A continuous fraction is convergent, if at least a limited number of denominators B_k vanish and if the limit*

$$x = \lim_{k \rightarrow \infty} \frac{A_k}{B_k} \quad (31)$$

does exist. In this case x is the value of the infinite continuous fraction. According to Pringsheim (1898) there exists an other convergence criteria: If for all $k=1, 2, 3, \dots$ the condition

$$|b_k| \geq |a_k| + 1 \quad (32)$$

is satisfied, the continuous fractions always tends to a finite, real limit.

Equivalence transformation of continuous fractions

Often continuous fractions contains partial denominators other than 1. Such and other continuous fractions can be transformed in new continuous fractions with arbitrary other partial denominators (or numerators as well) without changing the value x . Such a transformation is called **Euler's equivalent transformation**.

For this the continuous fraction

$$b_0 + \frac{a_1}{b_1} + \frac{a_2}{b_2} + \dots + \frac{a_k}{b_k} + \dots \quad (33)$$

is expanded by arbitrary real constants above or below zero $c_i \neq 0, i = 1, 2, \dots$ as

$$b_0 + \frac{a_1 c_1}{b_1 c_1} + \frac{a_2 c_1 c_2}{b_2 c_2} + \frac{a_2 c_2 c_3}{b_2 c_3} + \dots + \frac{a_k c_{k-1} c_k}{b_k c_k} + \dots \quad (34)$$

For an example we use the Global Scaling continuous fraction (6) with the numerators $Z_i = e$ and then transform it into a new continuous fraction with the numerators $Z_i = 1$. With application of (34) we find

$$\begin{aligned} N_0 + \frac{e \cdot 1/e}{|N_1 \cdot 1/e|} + \frac{e \cdot 1/e \cdot 1}{|N_2 \cdot 1|} + \frac{e \cdot 1 \cdot 1/e}{|N_3 \cdot 1/e|} + \frac{e \cdot 1/e \cdot 1}{|N_4 \cdot 1|} + \dots = \\ N_0 + \frac{1}{|N_1|} + \frac{1}{|N_2|} + \frac{1}{|N_3|} + \frac{1}{|N_4|} + \dots = \left[N_0; \frac{N_1}{e}, N_2, \frac{N_3}{e}, N_4, \frac{N_5}{e}, N_6, \dots \right] \end{aligned} \quad (35)$$

Many more transformations of continuous fractions or contractions are known, which we cannot discuss further. Only a short word is given to the Lagrange transformation which enables the transformation of a continuous fraction with positive and negative denominators into a continuous fraction with positive denominators only.

More about continuous fractions you find for example in books of Perron^[26] or Khintchine^[16].

4. The Muller Fractal

Exact Global Scaling continuous fraction

Now we are back on the Global Scaling continuous fraction. the complete formula is

$$\ln\left(\frac{X Z}{Y P}\right) = N_0 + \frac{e}{N_1 + \frac{e}{N_2 + \frac{e}{\ddots N_{L-1} + \frac{e}{N_L}}}} \quad (36)$$

with the elements

- X: Physical quantity or physical dimension
- Y: (super stable) calibration unit
- Z: Form factor
- P: Phase
- e: Partial numerator, Base of natural logarithm $e = [2; 1, 2, 1, 1, 4, 1, 1, 6, 1, 1, \dots]$
- N_0 : free member
- N_i : Partial denominator
- i: Scaling layer
- L: Length of continuous fraction

Physical dimension

A physical dimension represents – as it's name already says – a physical relevant, existent and somehow observable quantity or dimension. This quantity can be an arbitrary value from nature (mass, frequency, etc.) or a dimension in a construction etc. This physical dimension is the object for calculation together with a Global Scaling continuous fraction.

Each natural physical dimension can only be measured with a finite precision. Also man made constructions can only be produced with finite accuracy. For this reason, every physical dimension is represented with a value range for X. This range is bound by two **border values**. The lower border value is named **Min (or Inf** from infimum), the upper **Max (or Sub** from supremum). As a result, for each real physical dimension two Global Scaling continuous fractions are assigned, one for each border value X_{\min} and X_{\max} .

Calibration unit

The left side of a Global Scaling continuous fraction equation always contains at least an X value and a calibration unit Y. For sets of objects (or numbers) the calibration unit is $Y = 1$.

A part of its name the Global Scaling theory borrows from elementary particle physics. Again this is the case for the most stable calibration unit known. It is the proton's rest mass^[11]:

$$\begin{aligned} m_p &= (1.672\,623\,1 \pm 0.000\,001) 10^{-27} \text{ [kg]} \\ &= (938.272\,31 \pm 0.000\,28) \text{ [MeV]} \end{aligned} \quad (37)$$

The most commonly used calibration units and their computation is listed in appendix 2. As we see, also these calibration units have tolerances. Accordingly, as with the X values, a lower value Y_{\min} and an upper value Y_{\max} is assigned to the calibration unit Y.

The logarithmic line

The left side of the Global Scaling equation (36) – i.e. the value of the continuous fraction – is written as a natural logarithm of X and Y. Therefore please note that the value of the continuous fraction is not proportional to the value X of the physical dimension, but it is proportional to the logarithm of X. Hence, instead of writing about a linear number line, in Global Scaling we're dealing with a logarithmic number line, or simply a logarithmic line.

Denominators

A general continuous fraction would contain whole numbers except zero for the denominators N_i ($i = 1, 2, \dots$) only. In Global Scaling theory only a certain set of denominators are permitted.

- The free member N_0 is a whole multiple of 3. The value zero is possible.
- The denominators N_i are whole multiples of 3. The value zero is not permitted. Instead of using $-3, 0$ and 3 the values $-TZ-1$ and $TZ+1$ must be used (Where TZ is the numerator). This follows continuous fraction convergence criteria according to Pringsheim (32).

This rule of multiples of three is one of the outstanding characteristics of Global Scaling continuous fractions. This rule is derived from the group theory and shall not be explained in more detail. With this rule for denominators and for the free member N_0 , the logarithmic line is divided in sub-intervals. The free member N_0 causes gaps in distances of 3 on the logarithmic line.



Figure 8: Regular distance of 3 of N_0 on the logarithmic line.

There are some unoccupied areas on the logarithmic line because the denominators can only be set to certain values. When looking for the next lower scaling layers N_1 and N_2 we find the following graph around the point $N_0 = 3$ on the logarithmic line:

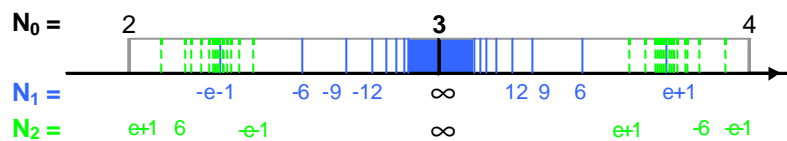


Figure 9: Hyperbolic distances because of $N_i \neq 3$ on the logarithmic line.

Only the **border values** for scaling layer N_2 are plotted in figure 9. For many layers we see, that larger gaps exist on the logarithmic line between $3n \pm 1$ ($n = \dots, -2, -1, 0, 1, 2, \dots$). If we repeat the same procedure for many more scaling layers, we will roughly get the following picture:

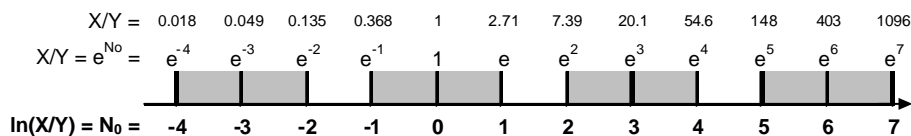


Figure 10: The linear chopping of the logarithmic line in the partial areas $N_i \pm 1$.

The logarithmic line gets intersected with gaps of wideness 1 in regular distance of 3. Also within the shadowed areas some smaller sub-gaps do exist. Again Figure 10 shows very clear, that a logarithmic line is used. The coefficient X/Y is plotted at the top of the graph.

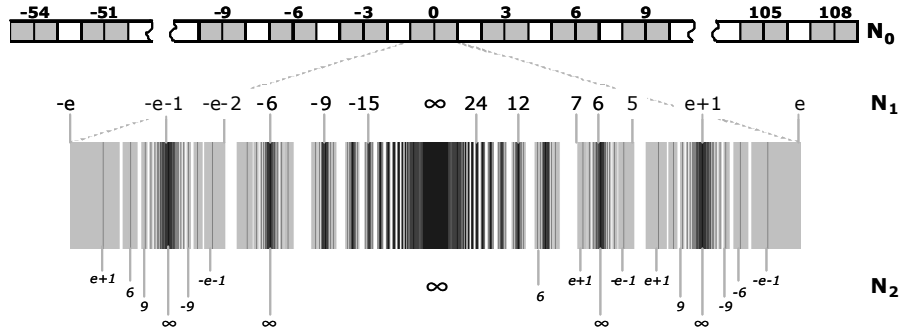


Figure 11: Hyperbolic chopping within the partial areas $N_i \pm 1$.

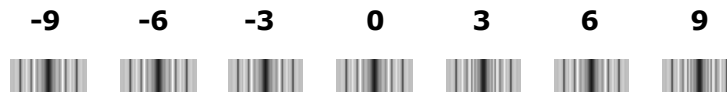


Figure 12: Regular and hyperbolic chopping of logarithmic line.

The distance and wideness of this sub-gaps around an area of $N_i \pm 1$ are not placed regularly in the logarithmic line. Now, on both sides of N_i the distribution is hyperbolic. This hyperbolicism is an inevitable consequence of the denominators N_i as a part of a fraction. Already figure 9 shows the creation of this sub-gaps very well.

Nodal points

Also these figures show, that the value of a continuous fraction does not change much with increasing values of the denominator ($N_i \rightarrow \infty$). The continuous fraction converges to a fixed value. In Global Scaling this value is called **nodal point**. At a nodal point $N_i = \infty$ the Global Scaling continuous fraction ends. Nodal points are possible on every scaling layer.

Usually in applications it is almost never the case that N_i get infinite. In most cases it is sufficient to terminate a Global Scaling continuous fraction calculation if $|N_i| > 1000$.

Border area

Each nodal value is placed in the hyperbolic middle of a valid section in the Muller set. Accordingly this section will have two borders. On the highest scaling layer N_0 this borders are placed at $3n \pm 1$, what is also shown in images 9-12. As long as the restrictions for denominators apply, this border values can never be reached exactly.

For example, to reach the border value of 4 on the highest scaling layer N_0 , we already see in figure 9 that

$$4 = 3 + \frac{e}{e+1 + \frac{e}{-e-1 + \frac{e}{e+1 + \frac{e}{-e-1 + \frac{e}{\dots}}}}}} \quad (38)$$

Hence, a border value can only be reached with an infinite length of the continuous fraction. Please note the denominator's sign alternation $e+1$ and $-e-1$ down the layers. The foresaid is valid for all scaling layers. If, for example, on scaling layer 2 the border value 7 must be, we get:

$$27 + \frac{e}{-9 + \frac{e}{7}} = 27 + \frac{e}{-9 + \frac{e}{6 + \frac{e}{e+1 + \frac{e}{-e-1 + \frac{e}{e+1 + \frac{e}{-e-1 + \frac{e}{\dots}}}}}}}} \quad (39)$$

A physical dimension, having at least partly such a structure, is also called **super-flexible**. If instead of border 7 the border 5 shall be reached, the denominators in corresponding layers change sign accordingly:

$$27 + \frac{e}{-9 + \frac{e}{5}} = 27 + \frac{e}{-9 + \frac{e}{6 + \frac{e}{-e-1 + \frac{e}{e+1 + \frac{e}{-e-1 + \frac{e}{e+1 + \frac{e}{\dots}}}}}}}} \quad (40)$$

Instead of writing this endless continuous fraction, it is also possible to end a continuous fraction just by setting the desired value to the denominator (see also equations (39) and (40)). Of course this exact value does not complain to the rules for the denominators anymore.

Abort criteria of Global Scaling continuous fraction calculations

The above described abort criteria also covers all which are possible. So we summarize them again. The Global Scaling continued fraction is aborted either

- at nodal value (super-stable physical dimension), or
- at a border value (super-flexible physical dimension), or
- in a gap or sub-gap value, or
- in a combination of them.

The termination of a continuous fraction analysis is always guaranteed due to the finite measuring tolerance of calibration unit Y and the finite accuracy of the X value. As a consequence in practice, the Global Scaling continued fraction is always finite.

The value of the lowest denominator N_L gives in Global Scaling theory some hints about the stability or tendency characteristics of a physical dimension.

Muller fractal

The Global Scaling continuous fraction and its associated rules quantize the logarithmic line and forms gaps and sub-gaps. The set of all possible values of a Global Scaling continuous fraction is called **Muller-set**, according to its inventor Hartmut Muller^[18]. This set can be plotted. The result is a Muller fractal. It has the following structure on the logarithmic line:

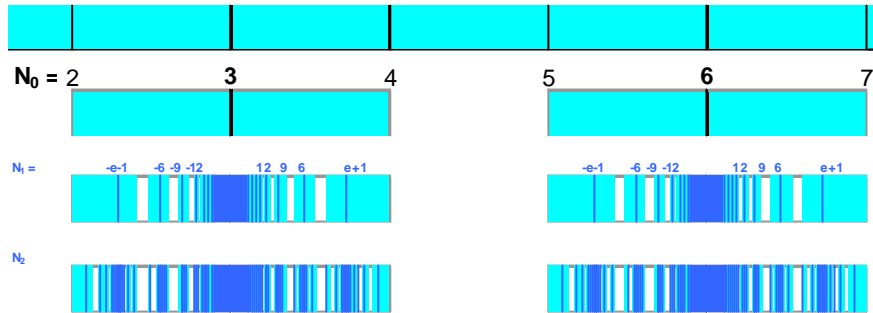


Figure 13: The structure of the Muller fractal on a logarithmic line.

This fractal strongly reminds to the Cantor set^[4]. Such a set is found by a recursion process, too. In difference to the Muller fractal, the Cantor fractal is built on a linear scale. To construct a Cantor fractal (named after George Cantor), we cut some parts out of the middle of a line segment.. This is repeated for all line segments (with the same relation of gap / remainder). As a result we get the Cantor fractal shown below:

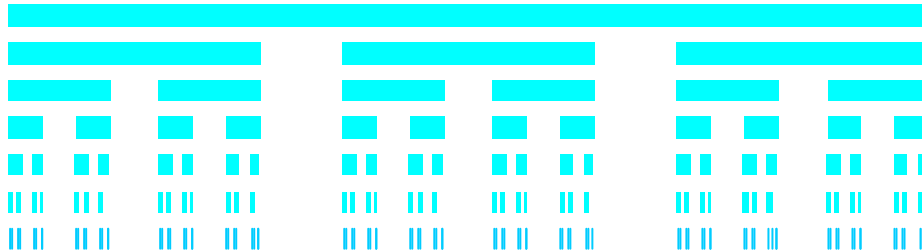


Figure 14: The structure of a Cantor fractal on a linear line.

The structure of a Muller fractal follows from the rule restrictions of the denominators used in a Global Scaling continuous fraction. Also the Muller fractal is constructed with a recursion process, namely with a finite Global Scaling continuous fraction. Consequently, the Muller fractal has a fractal dimension.

Fractal dimension

A fractal dimension has the general definition^[36]:

M shall be a partial set of the n -dimensional real number space \mathbf{R}^n ($M \hat{=} \mathbf{R}^n$). Now we cover this n -dimensional space with cubes having edges of length ϵ and count this cubes $N(\epsilon)$, which contains a piece of the set M . The limit

$$C = \lim_{\epsilon \rightarrow 0} \frac{\ln N(\epsilon)}{\ln \epsilon} \quad (41)$$

is named capacity C .

Beside the term *capacity* also the term **fractal dimension** or *Hausdorff dimension* is used. In case, where the edge length ϵ is limited by a finite value of a granular system, we can simplify the general definition(41) and find:

$$C = \frac{\ln N(\epsilon)}{\ln \epsilon} \quad (42)$$

For the Cantor fractal C is found to

$$C = \frac{\ln 2}{\ln 3} = 0.630929... \quad (43)$$

The Cantor fractal has not a whole but a broken dimension. Such a fractal (or set) is also called **strange**, if C is not a whole number. And strange sets always have gaps or holes. Hence, the fractal dimension gives some information about the fragmentation of a set. Let's view again to the earlier used beads. If all beads have the same size and are placed one by another without intersections, then a beads containing 1000 beads of 2mm diameter will reach a length of 2 meters. And the fractal dimension will become

$$C = \frac{\ln(1000)}{\ln\left(\frac{2\text{m}}{0.002\text{m}}\right)} = 1 \quad (44)$$

If the beads are not in contact with each other – the length of beads may be 3 meters – then the fractal dimension becomes now

$$C = \frac{\ln(1000)}{\ln\left(\frac{3\text{m}}{0.002\text{m}}\right)} = 0.944 \quad (45)$$

The fractal dimension is only then identical with a (geometric or topological) space dimension, if the set does not contain any gaps or holes.

The Global Scaling theory uses the model of an oscillating beads all the time. Because the Muller fractal has a broken fractal dimension, also the beads must have a finite distance in-between. This may give an additional descriptive picture about the fragmentation in the Muller fractal.

Influence of numerator to the Muller fractal

The numerator in a Global Scaling continuous fraction is a constant, but it must not necessarily be identical to Euler's number e for all continued fractions. Researches have shown that at least three different numerator values are applicable. The theoretical derivation of this three numerators cannot be given here. They have the following application:

- 2.0: Used for optimization of technical (or man made) systems
- e : Analysis of natural (long evolved) systems
- π : Used for prognosis (is not further described in this document)

Of course the Muller fractal changes shape in dependence of the numerator. Some subgabs become wider or narrowed.

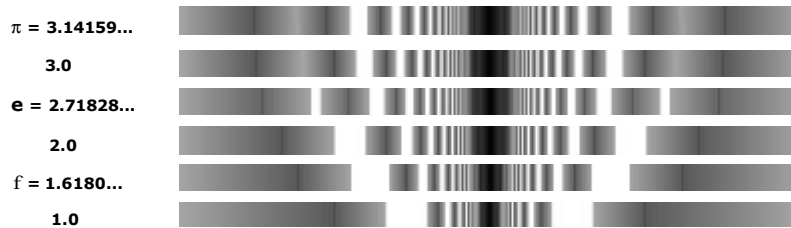


Figure 15: The influence of different numerators to the Muller fractal.

Working with the Muller fractal

Intensive and effective work with the Muller fractal for applications in research or development is possible only with a software tool having a graphic user interface and some automatic calculation routines. For this we recommend the software **GSC 3000 Enterprise** supplied by the [Institute for Space-Energy-Research GmbH \(IREF\)](http://www.aw-verlag.ch) in Wolfratshausen, Germany.

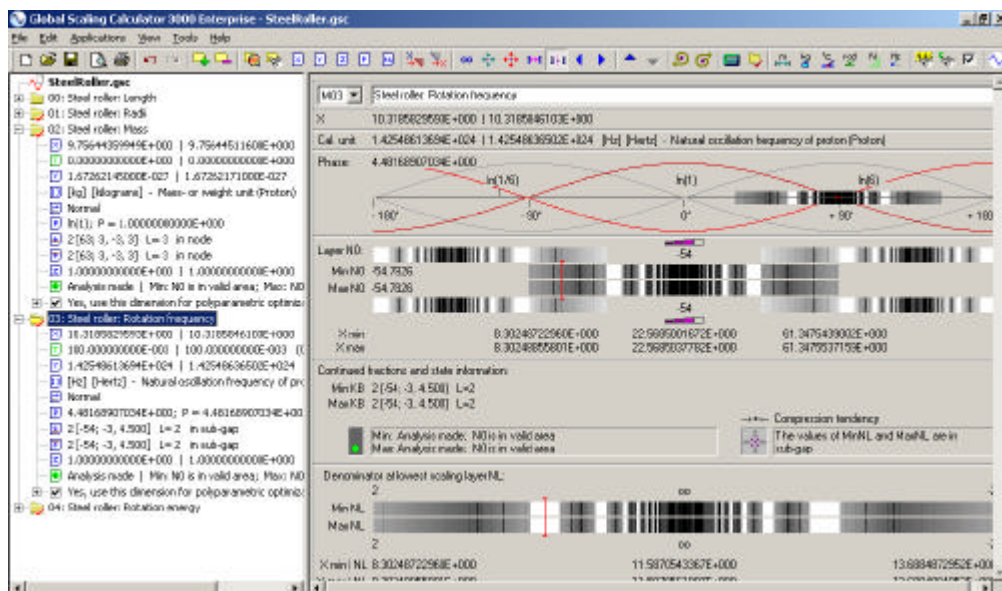


Figure 16: The graphic interaction with the Muller fractal with the software GSC 3000 Enterprise.

5. First physical interpretations

Standing gravity waves

The Global Scaling continuous fraction is derived from the model of an oscillating beads. In case of a mass line this model can be reused directly. The solution of Gantmacher and Krein^[11] has been derived for beads under two conditions:

- beads is oscillating freely at one of its ends
- beads is fixed at both of its ends

The Global Scaling theory assimilates the second model of the fixed beads. If such a beads is forced to oscillate, it's possible to generate **standing waves** on this beads, if certain resonance frequencies are taken. The wavelength of this transverse standing wave is in an exact whole relation to the length of the beads. Only between fixed „walls“ (or phase transitions) standing waves can occur, whereas the frequency is given by the distance between the walls und by the group velocity.

Experiments with standing (longitudinal) waves in a glass tube filled with a gaseous medium and small, light solid particles (cork powder) are well known. The standing wave oscillation transports the cork powder back and fourth and finally to the nodal points. The energy required is supplied by the standing wave. After some time no cork powder is left in antinodes.

■ Experiment of August Adolph Eduard Eberhard Kundt (1866)



Left: Experimental setup with Kundt's tube filled with cork powder.

Below: Applying a sine oscillation of 2700 Hz results in standing wave patterns. Please look at the fine structure!

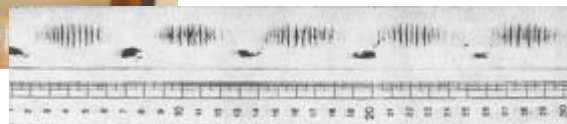


Figure 17: The experiment of August Kundt

With a standing wave the definition of a phase velocity makes no sense. The wave was build through reflections and is not propagating anymore. Mathematically it's therefore possible to speech of an infinite phase velocity. Physically this is not possible. Because the oscillating elements of the medium still have a rest mass, the phase velocity will never become infinite.

If a standing wave is disturbed from outside (for example we insert an other wall outside of a nodal point), the standing wave collapses because one of the conditions for a standing wave is not given anymore. Usually this collapse happens not simultaneous at all places but spreads with the finite phase- or group velocity of the wave.

This picture of a standing wave shall now be applied to our graviton medium. Over the universe's evolution a background field has been created. As a consequence, masses will be pushed away by antinodes and concentrate in nodal points. Generally this is the cause with gravity. Therefore, standing waves of gravitons are called **standing gravity waves**.

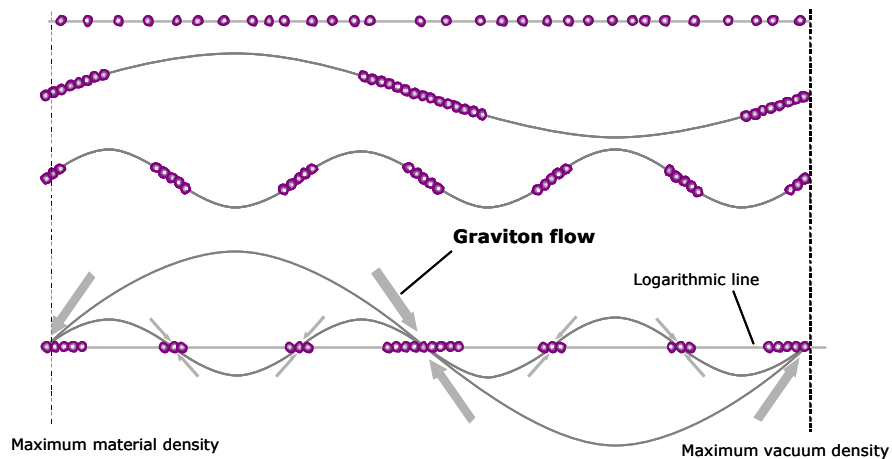


Figure 18: The effect of a superposition of several standing waves on a beads with freely moveable beads.

As we will see later, in Global Scaling the standing gravity wave is closely related to time. Anticipatory we can conclude, that in fact the standing gravity wave is not really a beads across the universe. This is only a heavily simplified but in some cases helpful model. Instead of dealing with a standing gravity wave, we can use the more precise description of a gravitative background field with all its short-time but synchronous fluctuations. This is in contrast to a common wave with a finite propagation velocity.

This synchronicity is well known and experimentally verified in quantum physics as the Einstein-Podolski-Rosen (EPR) effect for the microscopic cosmos. Additionally the Global Scaling theory predicts that also in macroscopic cosmos the same phenomena already exists.

Mass line

The logarithmic line of a Global Scaling continuous fraction (36) is theoretically of infinite length because mathematics does not predict some restrictions. Of course this changes when we apply some physical meaning to this numbers.

As said earlier, the most stable calibration unit in nature is the rest mass of the proton. An isolated proton has an average life time above $1.6 \cdot 10^{25}$ seconds^[11]. The particle with the closest life time is the free electron. It has an average life time of above $2.0 \cdot 10^{22}$ seconds^[11], or about one thousandths of proton's life time. The third atomic particle – the neutron – has in unbounded state just an average life time of only 896 seconds^[11], which is comparatively nothing.

Because of its outstanding stability, the proton rest mass is the basic calibration unit Y_p in Global Scaling theory. A number line calibrated with the proton rest mass is called a **mass line**. With this calibration on the logarithmic line, each value on this line corresponds to a real physical value, in our case to a mass X .

Muller^[23] identified the smallest possible masses on the logarithmic line at the place of $N_0 = -54$. This corresponds to the photon or graviton rest mass m_γ , i.e. the rest mass of the medium quanta. This value is so small that we cannot detect it with today available measurement technologies:

$$m_\gamma = e^{-54} m_p = 5.908 \cdot 10^{-51} \text{ [kg]} \quad (46)$$

This value constitutes the lower end of the mass scale. The upper end m_H on the logarithmic line is given by the value $N_0 = +189$. Theoretically this value corresponds with the total mass of the universe and is

$$m_H = e^{189} m_p = 2.018 \cdot 10^{55} \text{ [kg]} \quad (47)$$

In-between we have fractal intersections on the logarithmic line according to the Muller fractal. The kilogram of Paris is approximately in the middle of this two extremely values (based on \log_{10} not \ln). The logarithmic line contains 3^*81 main sections. This main section can be divided by 3 many times, because it is $1\cdot3\cdot3\cdot3=81$. The values of the mass line are listed in appendix 3.

Graviton flow

The oscillating medium (i.e. our universe) consumes energy to cover its losses and to preserve the created structures. Consequently our universe is an energetic open system where an energy inflow takes place all the time. In standing waves an energy in- or outflow without destroying the wave is only possible at nodal points. Therefore, the periphery of the universe is interpreted as a nodal point, too.

With the oscillation of the beads (or the medium with the embedded masses) all masses are pushed to the nodal points. There the pressure is higher than at antinodes. For example the Earth is located in such a nodal point. Additionally a steady flow of gravitons or small masses happens toward the nodal points. As a result, the mass in the nodal point – in our case the Earth – is growing.

The closer to a nodal point, the higher (or faster) or the graviton inflow. The resulting gradient vector is equivalent to the time (more later). Again we note a counteraction between gravity and time.

Compression and decompression (fusion and decay)

Because of the mass increase, a mass travels on the logarithmic line slowly to the right (upwards). As a result the mass undergoes alternately fusion- and decay-tendencies. The mass travels on arbitrary scaling layers and from border values to nodal points and beyond, always upwards on the logarithmic line.

The higher a scaling layer is, the higher is a possible impact, priority or effect an event will have to other systems. If for example a mass traverses a nodal point on scaling level N_{10} , the expected influence to other masses or to the mass itself is rather small. Such a jump can just happen if a planet catches a small particle. But this will become more critical for the mass itself, if the value comes to a border line on highest scaling layer.

If a mass has had a fusion tendency up to the traveling to next nodal point, this will change to decay tendency after passing this nodal point. The more a mass travels to the right – according to its growing mass – the more distinct is the decay tendency. When reaching the right border on N_0 , the mass either accumulates rather faster mass particles to “jump” to next valid area or the mass will decay to smaller pieces. This smaller pieces now are again shifted more to the left on the logarithmic line and can start traveling to the right again.

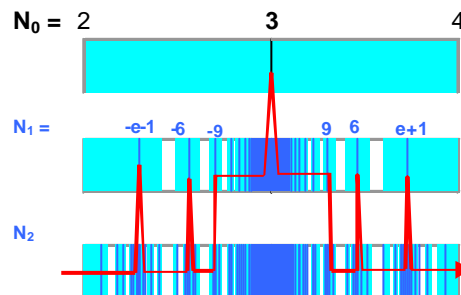


Figure 19: The traveling on the mass line.

Such transitions where a mass does not manage this „jump over the gap“ are well known. One example is the natural radioactivity (decay of atomic nucleus). Others examples are exploding stars (novae, super-novae). Although this decomposition must not happen explosively, it also can take place very slowly as simple radiation. Because of the inverting characteristics of the scaling layers, the simple structure as shown in Figure 19, is not fully correct:

- For N_0, N_2, N_4, \dots we have fusion tendency on the *left* side of node and decay tendency on the *right* side of node.
- For N_1, N_3, N_5, \dots we have fusion tendency on the *right* side of node and decay tendency on the *left* side of node.
- The priority of the tendency is determined by the scaling layer level.

Additionally the reader shall be warned that an other exchange of fusion- and decay-tendency takes place in case of an inversion of the whole logarithmic line. This is the case if an increasing value on the logarithmic line does correspond with energetic decreasing values and vice-versa.. Example: The higher the frequency, the higher is the energy equivalence. The logarithmic line is energetic increasing. But the higher the periodic duration, the lower is the energy because we have $T = 1/f$. Then the logarithmic line is energetic inverted. Generally for the different sections in a Muller fractal for upward energetic direction we have the following classification:

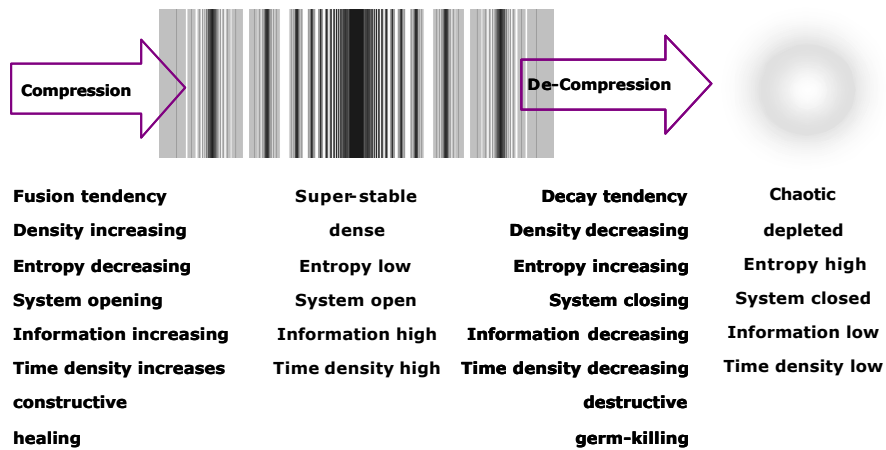


Figure 20: Qualitative information about the different sections within a Muller fractal.

The higher the scaling layer, the higher is the priority and the expected effect on the affected physical dimension. Just to repeat: the fractal is only symmetric when plotted for the highest scaling layer and when plotted on a logarithmic line. To visualize this, we see on the next figure the projection of the Muller fractal to a linear line. This transformation clearly indicates the two main sections of compression (left) and decompression (right).

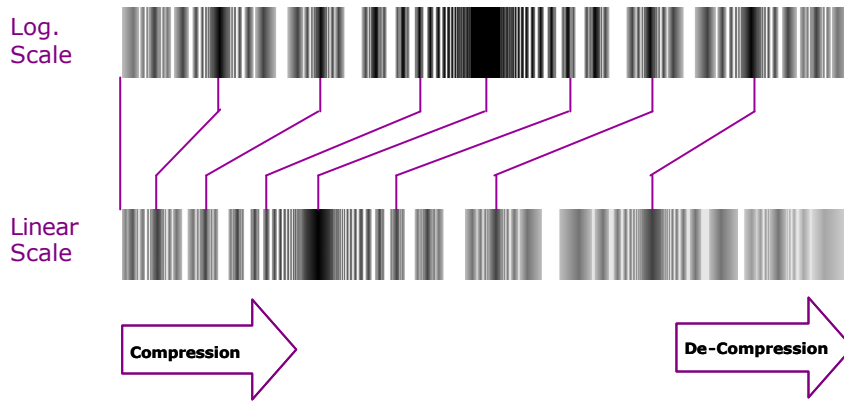


Figure 21: The projection of the Muller fractal from a logarithmic line to a linear line.

Phase on the logarithmic line

The attentive reader will recognize, that by calculating the mass line many natural masses fall into a gap or sub-gap area of the Muller fractal. A prominent candidate is for example the electron rest mass^[11].

$$\begin{aligned} m_e &= (9.109\,3897 \pm 0.000\,005\,4) \cdot 10^{-31} \text{ [kg]} \\ &= (510.990\,06 \pm 0.000\,15) \text{ [keV]} \end{aligned} \quad (48)$$

or the mass of Earth^[11]

$$M_E = (5.976 \pm 0.001) \cdot 10^{24} \text{ [kg]} \quad (49)$$

Both masses lie into a gap of the Muller fractal. The electron rest mass lies between the border values -8...-7 of the free member N_0 , the mass of Earth between 118...119. Only with the introduction of a new quantity – the so called **Phase P** – this values can be cast within the Global Scaling continuous fraction (36). Correspondingly we find on the left side of the Global Scaling continuous fraction a placeholder P to use for the Phase. According to Global Scaling theory the Phase P adopt especially three different values:

- P = 1 (no shift)
- P = 4.481689 (shift of +90° on the logarithmic line)
- P = 0.22313 (shift of -90° on the logarithmic line)

The last two phase values corresponds with congruent fractals. (please note that the distance between two nodes of a standing wave is one half of the wavelength or 180°). Now the logarithmic line looks like:

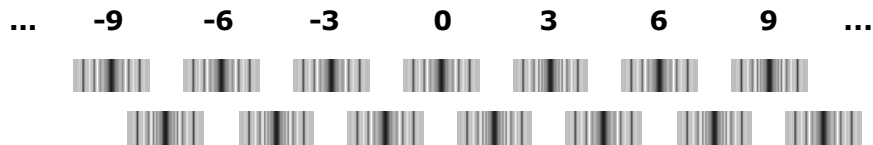


Figure 22: The two Muller fractals shifted by 90° against each other. This shift corresponds to 1.5 logarithmic units on the logarithmic line.

This phase values must always be taken into consideration for calculations according to Global Scaling. This two group of fractals can also be characterized as:

- No shift: Vacuum compression wave
- With shift: Mater compression wave

Beside this two other natural phase shifts are known, which apply to long evolved natural quantities (as for example elementary particles):

- $P = 6$
- $P = 1/6$

Technical or man made systems which are not long evolved or do not have a century old tradition usually have all other kinds of possible phase values. To perform a Global Scaling optimization this phase value **MUST** be found for a particular application by careful data collection and analysis. The software **Global Scaling Calculator 3000 Enterprise** has implemented some very useful tools to find the most likely phase out of a data set.

Critics may now argue that with an „arbitrary“ phase every desirable X value can be assigned to every possible continuous fraction, or the other way around, for each continuous fraction a desirable X value can be adjusted. Mathematically this is correct, but not from an application specific point of view. The current Global Scaling know-how indicates, that for each single application only one relevant phase can be identified as unique.

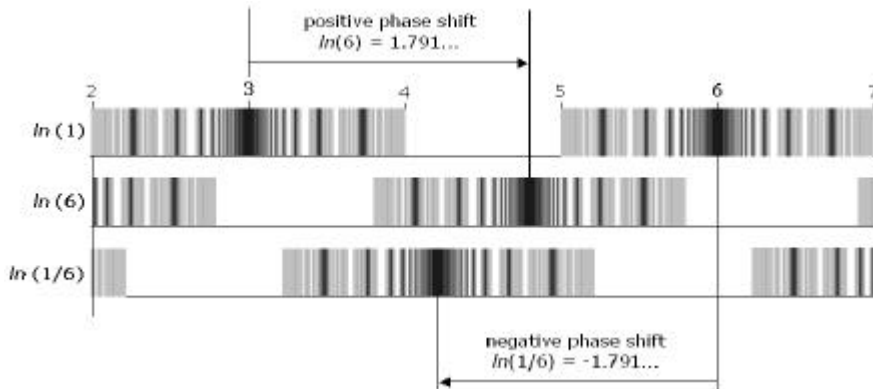


Figure 23: Phase shift on a logarithmic line

At this point we shall again point to the fact that the Muller fractal describes the **probability** to find a certain value in the region of a nodal point. Obviously there will always be some values which are placed in the low-probability region of a gap (see also figure 1 of Cislenco), but in general more values fit into nodal point regions than into gap regions.

To explain the phase shift of 6 and 1/6 Muller^[23] uses the model of reflection of gravity waves at the ‚edge of the universe‘. But – as noticed earlier – the wave model is only a simplified didactic model, therefore the value of this explanation is more didactic than reality. But this simple model helps to understand why phase shift may occur. On every region with differences in graviton density, a wave is at least partly reflected. It follows straight forward that this leads to local standing wave effects which could indeed have any phase value. Interestingly the wave model can also be applied to the pure mathematical number line (which gives by the way the distribution of prime numbers). So also the pure number is „oscillating“ and of course this is then visible in all sets of things. Finally, instead of phase shift Muller sometimes also speaks of **channels**.

The phase shift relativizes some statements that nature has some hard definable, preferred regions whereas other regions will be avoided. Because of this parallel channels – or parallel multi-fractals on the logarithmic line – basically all values can be realized in nature. But with the selection of the phase a system decides which values are preferred and which not. Once a decision has been made by nature, it does not change this phase easily. And this gives a chance to optimize technical systems according to observable phases and numbers in nature.

Now, with the phase shift we are able to calculate the rest mass of the electron with the rest mass of the proton, which is (approximate)

$$\ln\left(\frac{m_e}{m_p} \frac{1}{6}\right) = -9 + \frac{e}{-9 + \frac{e}{18 + \frac{e}{\pm 671}}} \quad (50)$$

The lowest denominator N_3 follows from the tolerance of the measured values m_p and m_e and is – according to the **Global Scaling Calculator 3000 Enterprise** – exact ± 671 . That means, the lower limit is -671 and the higher limit is $+671$. This indicates, that not many scaling layers are necessary to come close to the measuring uncertainty or calculation rounding errors. Because of this very high symmetry we can define the average value of the electron's rest mass with $N_3 \rightarrow \infty$ and we find:

$$\ln\left(\frac{m_e}{m_p} \frac{1}{6}\right) = -9 + \frac{e}{-9 + \frac{e}{18}} \quad (51)$$

This continued fraction for the electron is also given by Muller^[23]. Muller names this kind of continuous fractions *super-stable*. Physical dimensions having a super-stable continuous fraction are – as its name already says – long living and very stable.

Super-stability

Muller has used first the term super-stability in 1982^[18]. Global Scaling continuous fractions which follow the **strong criteria** of super-stability, are characterized as follows:

- All denominators together have a cross sum equal to zero.
- All denominators and the free member are a whole multiple of 9.
- The length of the continuous fraction is exactly $L=2$.

An additional **weak criteria** claims that all denominators should values as lowest as possible. As we have seen with the electron rest mass calculation, these criteria can be applied independent of the current phase shift.

If we take a look at the continued fraction of Gantmacher-Krein (5) for an oscillating beads, we recognize that the shortest possible continuous fraction requires a minimum of three denominators (including free member) to enable the oscillation of one single bead. This can be put forward to the electron and we find the equivalence of:

$$\ln\left(\frac{m_e}{m_p} \frac{1}{6}\right) = -9 + \frac{e}{-9 + \frac{e}{18}} \leftrightarrow l_1/\sigma + \frac{1}{-m\omega^2 + \frac{1}{l_0/\sigma}} \quad (52)$$

The sum of the free member N_0 and of the denominator N_2 corresponds with the length of the beads divided by its mechanical tension, which is assumed as constant throughout the whole beads. The denominator N_1 is equivalent to the product of mass and resonance frequency.

It's clear that a super-stable, natural quantity must contain a minimal number of oscillating masses. The more complex a system is, the lower is the probability that an oscillation keeps stable and therefore the higher is the chance that a system becomes unstable and decays.

The high accuracy of the calculated value with the measured electron rest mass is astonishing. But the theory in the given form does not answer the question why just this continued fraction is so stable and not an other one. A look into table of appendix 4 indicates, that there may exist more theoretical hints about that.

Length line

Until now we have applied to logarithmic line to masses. As stated earlier, it can be calibrated with arbitrary calibration units. Therefore let's have a look at the length line. For this we calibrate the line with Compton's wave length of the proton (also refer to appendix 2)

$$\lambda_p = \frac{h}{2\pi \cdot c \cdot m_p} = (2.103\ 089\ 3 \pm 0.000\ 002\ 5) \cdot 10^{-16} \text{ [m]}, \quad (53)$$

where h is Planck's constant and c is the speed of light in vacuum. The length line is plotted in appendix 5 together with numerical values using no phase shift. By the way, the arrangement of biological organisms on logarithmic scales is known very well.

The length line is 'shorter' than the mass line. It starts also with $N_0 = -54$, but ends earlier at $N_0 = +108$. Also the length line can be divided in sub-sections of 3, because we have $108+54 = 164 = 2 \cdot 81 = 2 \cdot 3 \cdot 3 \cdot 3 \cdot 3$.

Modes on the logarithmic line

This dividing into 3 parts of the mass- or length line reveals on other basic pattern of the logarithmic line. Whereas the Global Scaling continuous fraction uses already a quantum of 3, also all physical value range is a multiple of this factor 3.

In the figure below the four oscillation **modes** on the logarithmic line are clear visible. This can also be interpreted with overtones in the model of the oscillating beads. These modes k have the simple rule 3^k and correspond therefore to the series 3, 9, 27 and 81 units on the logarithmic line.

Each of this mode is similar to a sine wave on the beads. Accordingly the gravitons are denser at nodal points than at antinodes. This different density zones along the logarithmic line create **structural changes** of objects placed along this line.

With a length line the most dense point is at $N_0 = +27$. There all modes have their nodal point. Between this nodal points physical interactions take place.

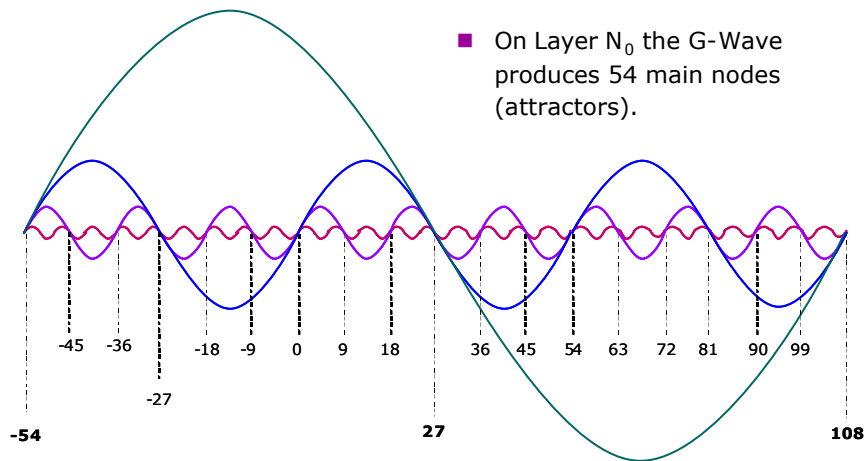


Figure 24: The four oscillation modes of the G-wave

These modes we find again in the relation of different natural structures. Some cosmic structure ratios are listed below.

$\frac{\text{Avg. Distance between stars}}{\text{Diameter solar system}}$	$= \frac{10 \text{ Light years}}{11.6 \cdot 10^9 \text{ km}} \cong 8100 = e^9$
$\frac{\text{Diameter solar system}}{\text{Diameter Sun}}$	$= \frac{11.6 \cdot 10^9 \text{ km}}{14000000 \text{ km}} \cong 8100 = e^9$
$\frac{\text{Distance between galaxies}}{\text{Diameter of our galaxy}}$	$\cong 20 = e^3$
$\frac{\text{Diameter galaxy clusters}}{\text{Diameter of our galaxy}}$	$\cong 400 = e^6$
$\frac{\text{Diameter Eunasto cells}}{\text{Diameter galaxy clusters}}$	$\cong 20 = e^3$
$\frac{\text{Diameter super-clusters}}{\text{Diameter galaxy clusters}}$	$\cong 400 = e^6$

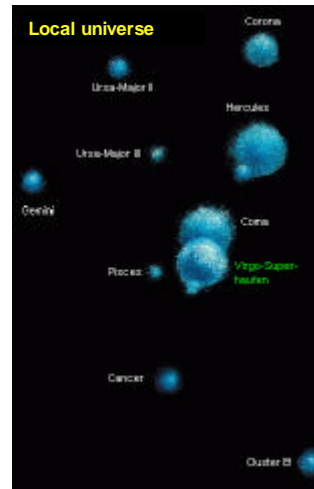


Figure 25: Some cosmic structure relations

If we look for similarities between objects of far distant size, these modes are very important. For example the proton is located at the node $N_0 = 0$. Interestingly the brain frequency (about 5 Hz) is in the node -54 (the frequency line follows next). This is a logarithmic distance to the proton of 2×27 . In the length line, the proton in turn has a logarithmic distance of 27 to the very important 27, which occupies the region of the DNA.

Frequency line

With the same procedure as shown for mass- or length line we can calibrate the frequency line. The calibration unit is:

$$f_p = \frac{2\pi \cdot c^2 \cdot m_p}{h} = (1.425\,486\,1 \pm 0.000\,001\,7) \cdot 10^{24} \text{ [Hz]} , \quad (54)$$

The frequency line gives unambiguous values. Very interesting is for example the area of visible light^[24]. The visible light occupies the border range at $e[-21; e-1]$. The dangerous UV-C radiation is on the left side of the node $N_0 = -21$ on the highest scaling layer. And exactly next follows the UV-B and finally UV-A (see next picture).

Men's eyes, the green of leaves and most of the living creatures are specialized to the wavelength of the green light. The reason lies in the color spectrum of the sun light. This spectra (equivalent to a black body radiation with a surface temperature of about 6000K) has its maximum value at green color. This green color lies exactly in the node $-e-1$ on scaling layer N_1 .

The red color marks the end of the border area at $N_0 = -22$ or $e[-21; -e-1, e+1]$. The following gap is the range of thermal radiation. The violet marks the other end of the border area at $e[-21; e+1, -e-1]$ and finally it changes at node $N_0 = -21$ to ultraviolet radiation.

The value range of the frequency line is inverse to the range of the length line. Therefore the lowest possible value for N_0 is -108 , the highest possible value is $N_0 = +54$. Of course also here we find the same modes $108+54 = 162 = 2*3*3*3*3$ as discussed with other lines. The frequency value table is listed in appendix 6.

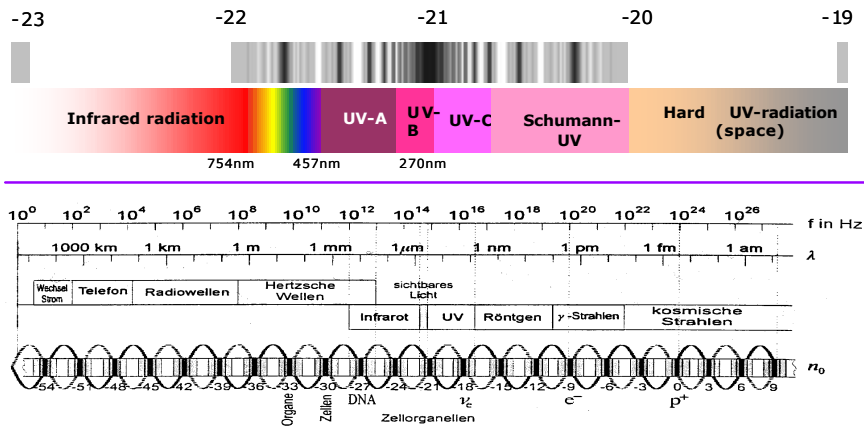


Figure 26: The electromagnetic spectra in the range of visible light.

Time line

Finally we have a look at the very important time line. The calibration unit is the inverse of the frequency calibration unit:

$$\tau_p = \frac{h}{2\pi \cdot c^2 \cdot m_p} = (7.015\,150\,8 \pm 0.000\,008\,4) \cdot 10^{-25} \text{ [s]}, \quad (55)$$

Now the time line cannot be used as directly as it's the case with the frequency line (except for oscillation periods). The calibration unit as an inversion of Hertz is seconds. This is – rigorous interpreted – only valid for oscillating systems because the derivation was made via the protons Compton wavelength which in turn is an oscillation value. For such processes this time line is very useful (i.e. oscillation periods, circulation time, orbits). Again the value range of the time line is inverse to the frequency line or similar as with the length line and goes from $N_0 = -54$ to $N_0 = +108$.

With our habit to record the past and predict the future, we have a certain location on the cosmic time line. But which place should it be? A prognosis for the development of a single value according of the time line is theoretically possible, but practically we have a heavy problem. We do not know exactly at which position in the cosmic time line we are right now. But for a prognosis it is indispensable that we set the time line according to our present.

6. Time

The description about different logarithmic lines (or *dimensions*) given so far shows a simple overview about calibrated Muller fractals. One would like to conclude that nature only tends to realize values outside of the gap areas of the Muller fractal. But as we have discussed in previous sections, this is not true in general. Therefore the questions arise what else interpretations do exist for the Global Scaling continuous fraction and how can it be used for interpretations of exceptional experiments or for prognosis of new effects – as for example for gravitation.^[47] or energy generation. The essence of time is an important key of a new physics. Let's have now a closer look to the dimension of time.

Global time wave

The standing gravity waves create zones with different densities along the logarithmic line. Again we recall the foresaid, that in fact the logarithmic line does not really exist as a physical standing wave in general, it only enables under some circumstances the local creation of standing graviton waves. But this pictorial model is useful to understand the **natural selection processes**, which finally leads to the variety of objects and life forms, as we know them today.

Because of the concentrative gravity effect and of the resulting graviton inflow to the nodal regions, the medium is not **homogenous** and not **isotropic**. Non-homogeneity follows from the several different density zones, non-isotropic follows from the orientation of graviton flow in space.

Because of this steady graviton flow all masses always tend to growth. Also Earth – as other planets – is continuously growing. This idea is not new and has been published long ago several times, as for example by Walter Russell^[30]. Similar to the drift of points on an inflating balloon we can observe the drift of continents and the associated seduction zones under the world sea.

Around Earth we have a steady graviton inflow towards the center. This is the cause of gravity force. The flow velocity is not constant and decreases with growing distance from Earth surface. This gives a gradient of the velocity field or of the graviton density. The gradient will be non-zero because the graviton field around Earth is not isotropic. The amount of the gradient field is increasing towards the nodal points.

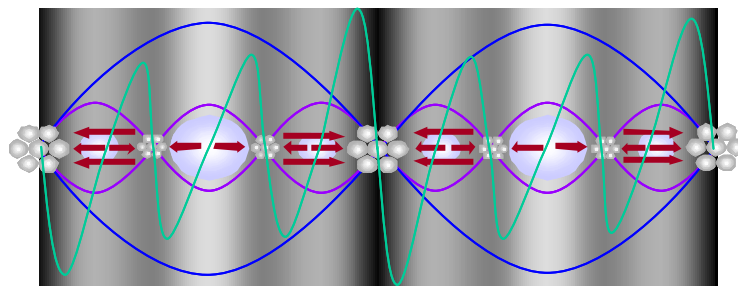


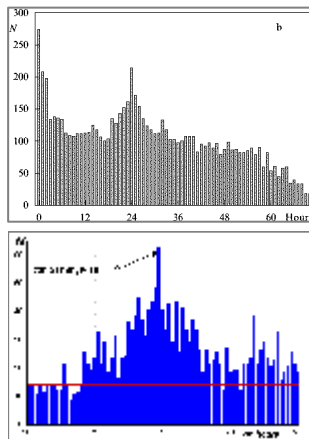
Figure 27: The gradient of graviton velocity (green line) in a small section of the Muller fractal.

This gradient vector creates the local effect of time flow. Or more precise: **Time is the gradient of the graviton density**. This Global Scaling theory^[24] definition is very fundamental and cannot be deduced theoretically. It follows immediately that time must have the same fractal properties as the Muller fractal for example applied to the mass line. Time emerges to a real observable physical dimension with qualitative and quantized properties. The global standing gravity wave expands and compresses the local time in logarithmic-hyperbolic intervals. In analogy to the global standing gravity wave, this is the **global time line**.

In the section about recursion we have seen that a simple loop (on a certain scaling layer) can only be repeated several times, if this repetitions happens in sequence (not simultaneous). Then the output also changes in steps as well as the processing time proceeds in steps. In general this result together with the known structure of the Muller fractal leads to the conclusion, that time does not flow continuous but in certain steps. Time flow is quantized. This can be tested experimentally.

Experiments of Shnoll et. al.

More than 40 years ago a Russian research team around Professor Simon E. Shnoll^[35] discovered discrete reaction velocities in biological processes, namely the hydrolysis of muscle proteins Myosin and Actomyosin. Then, after successful control experiments they expanded the research to chemical reactions as the famous Belousov-Zabatinsky-Oscillation and finally they analyzed random physical processes as for example the natural radioactive β -decay of Carbon ^{14}C . And all the time the scientists concluded that *„It is shown that due to fluctuations, a sequence of discrete values is generated by successive measurement events whatever the type of the process measured. The corresponding histograms have much the same shape at any given time and for processes of a different nature and are very likely to change shape simultaneously for various processes and in widely distant laboratories. For a series of successive histograms, any given one is highly probably similar to its nearest neighbors and occurs repeatedly with a period of 24 hours, 27 days and about 365 days, thus implying that the phenomenon has a very profound cosmophysical (or cosmogonic) origin.“*



Sorting of similar histogram pairs according to their distance in time. Some unexpected accumulations can be observed.

← Measuring of radioactive β -decay of ^{14}C

← Measuring of radioactive α -decay of ^{239}Pu in Puschino (Moscow) and of α -decay of ^{228}Ra in Lindau (Germany)

Figure 28: Two histogram analysis results made by Professor Simon Shnoll (Source: Physics- Uspekhi and Physics and Chemistry of the Earth).

What the researchers have made? First they collected a huge amount of measuring data and transformed them to histograms. A **histogram** shows a group of probability distribution of a set of measurement values. A finite but high amount of data is required to plot a histogram. These vales are sorted according amplitude and then are grouped to classes of comparative sizes (similar to group together potatoes of a certain size). The number of class elements (number of potatoes on huddle) is now set into relation of the total number of measurement values (total number of potatoes) and as a result we get the probability distribution. To get a more or less precise histogram, about thousand measurement values should be taken into calculation.

Shnoll et. al. have recorded so many measurement values, that they were able to plot several consecutive histograms. The first histogram bases on the first 1200 measuring values, the second histogram the next 1200 measurement values and so forth:

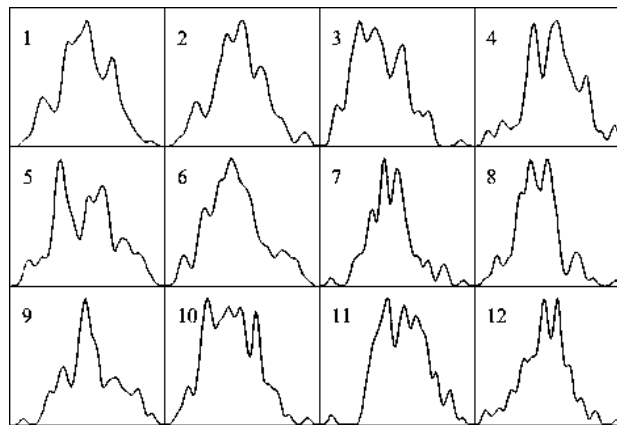


Figure 29: A sequence of 12 consecutive histograms (Source: Physics-Uspekhi)

With a software tool, the scientists put together a sorted long line of such histograms. Now they started to search for this histogram pairs, which appears to be of most similar shape. The result will be as follows:

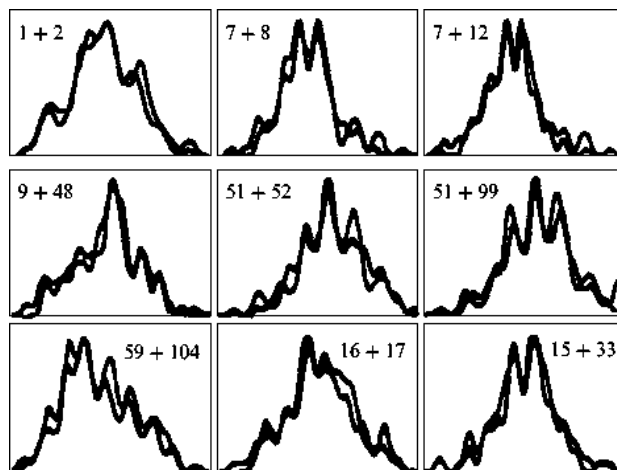


Figure 30: Sorting of most similar histogram-pairs (Source: Physics Uspekhi)

This sorting process was done by software also. Then a time analysis was performed. Because every histogram marks a certain section in recording time it is possible to calculate the time difference between this most similar histograms. If, for example, every second a measuring value is recorded, a histogram represents an elapsed time of 1200 seconds = 20 minutes and so on. Now, the most similar histogram pairs are put together (see Figure 30) and it is possible to find the time in-between this two histograms. Finally they sorted the distribution of the histogram pairs along the time axis. For pure stochastic processes it's commonly expected, that the similarity of histogram-pairs does not show significant differences. But the result of Shnoll et. al. gives an other picture:

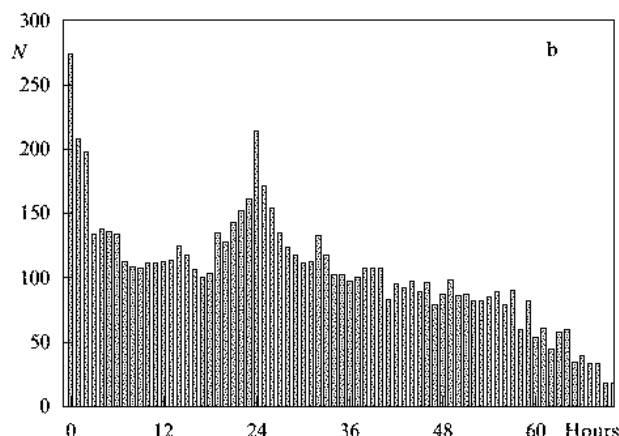


Figure 31: Distribution of time intervals between most similar-shaped histogram-pairs
(Source: Physics Uspekhi)

As expected the nearest histograms in time are very similar in shape, but beside this the figure shows again a clear maximum after 24h. A similar pattern can be recorded after 27.28 days and after 364.4, 365.2 and 366.6 days. The first value is exactly the moon's orbit time, the middle value of the second group corresponds with the sidereal year, which is the exact earth orbit around the sun.

But there is more. If the Shnoll experiments were recorded at the same time but at different locations, the histogram analysis gives very similar results, independent whether the same or different physical or chemical processes have been measured.

About more than two years this publication of Shnoll et. al.^[35] has not been commented and probably in Western science nobody took notice of it. But the critics cannot invalidate the main claims of Shnoll's paper. Then, in 2000 Shnoll et. al. published a new paper and summarized their findings as follows^[36]

1. *The fine structure of the distributions governing the results of simultaneous measurements of **any** process in each time interval is similar with a fairly high probability. This similarity is observed even when the labs are hundreds or thousands of miles away from one another. The similarity of histogram shapes cannot be attributed to any artefacts, because the experimental setups are totally independent, and sometimes there occurs principal difference even in the method of measurements.*
2. *The shape of histograms is reproduced with a high probability in adjacent time intervals (the effect of 'close neighbours'), and is repeated with a periodicity of 24 hours, 27 days, and 1 year.*
3. *From statements 1 and 2 it follows that the phenomenon under discussion is caused by cosmophysical factors..*

If the reader likes to compute similar histogram analysis by Shnoll with his own data sets, we recommend the software **Global Scaling Calculator 3000 Enterprise**.

Finally there is an other picture summarizing the above statements:

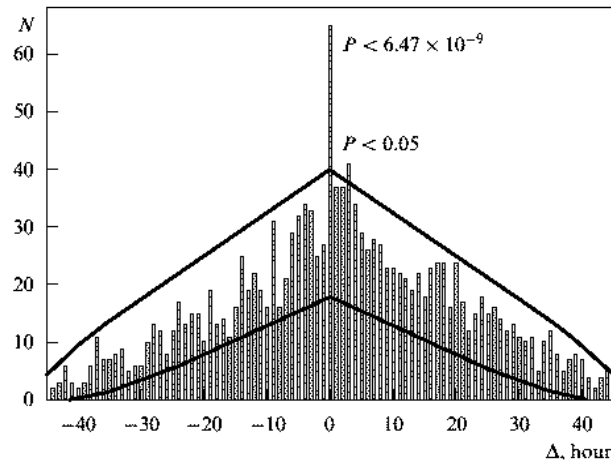


Figure 32: Synchronicity of simultaneous measurement of α -decay of ^{239}Pu in Pushchino (Moscow) and of β -decay of ^{137}Cs in Dubna. Shown are the number of pairs N of similar histograms and the corresponding time of occurrence in minutes. The most probable situation describes the simultaneous appearance of similar histograms from both different physical processes. (Source: Physics Uspekhi)

Kozyrev's concept about the properties of time

„Time is the most important and most enigmatic property of nature.“ With this statement a almost unknown paper of Nikolay Alexandrovich Kozyrev^[17] starts. And as we shall see, this is not an overstatement. His theory bases on three axioms:

1. Time possesses a quality, creating a difference in causes from effects, which can be evoked by directivity or **pattern**. This property determines the difference in the past from the future.
2. Causes and results are always separated by space. Therefore, between them exists an arbitrarily small, but not equaling zero, spatial difference.
3. Causes and results are separated in time. Therefore, between their appearance there exists an arbitrarily small, but not equaling zero time difference of a fixed sign.

The second axiom is equivalent to Newton's infinitesimal calculation ($\partial x \neq 0, \partial t = 0$), the third axiom is just the opposite. In atomic physics we have the inverted situation. Because of the uncertainty principle the superposition of fields is possible with $\partial x = 0$ and $\partial t \neq 0$. Thus classical mechanics and quantum mechanics mark both ends of the general case

$$\frac{\partial x}{\partial t} = C_2 . \quad (56)$$

C_2 has the dimension of a velocity. It's a kind of causal-resultant relationship and shows "how fast" the transmission of cause to effect in space and time occurs. In a real world it's $C_2 \neq 0$. But in classical mechanics we have $C_2 = \infty$ and in quantum mechanics it's $C_2 = 0$. The symbols ∂x and ∂t denote the distance between cause and effect. Consequently C_2 is not a property of bodies but of the intersecting space.

The positive direction of time – and therefore the sign of ∂t – is always the future minus the past. The sign for ∂x is not defined so clearly. But the causal direction of C_2 should still be unique. So we can find a vector \mathbf{i} for the resulting causal direction as

$$C_2 \mathbf{i} \partial t = \partial x . \quad (57)$$

The time pattern must be set in relation to a fixed frame. This cannot be the position of any material point. What's left is the empty space. And space is able to distinguish between



left and right (symmetry breaking). This symmetry breaking is well known in quantum physics for particles having spin. In a right-handed coordinate system the time pattern is positive, in a left-handed coordinate system negative (mirror image). Therefore Kozyrev suggested that C_2 corresponds with a physical rotation velocity. Accordingly he conducted many experiments with gyrators and later with reflecting walls.

Kozyrev said: „Time enters a system through the cause to the effect. The rotation alters the possibility of this inflow, and, as a result, the time pattern can create additional stresses in the system. The additional stresses alter the potential and the full energy of the system. These variations produce the time pattern. From this it follows that time has energy. Since the additional forces are equal and are directed oppositely, the pulse of the system does not vary.“

In a left hand system Kozyrev measured the following approximate value for C_2 as:

$$C_2 = +700 \pm 50 \quad [\text{km/s}]. \quad (58)$$

Experiments with vertical rotating gyroscopes of 90g with left rotation shows a weight reduction for of -4g and for a right rotation a weight increase of +4g. Additionally, experiments with several pendulum and fall tests show a slight deviation to South pole. If the masses are subject to an additional vibration process, even an other force can be observed, which does not vanish immediately after stopping the vibrations but slowly reduces back to zero with a half-life time between 11...70 seconds. This additional force always causes a weight increase of the vibrating mass. The best experimental results Kozyrev obtained in spring and autumn, whereas in summer und winter the effects are not as significant.

With torsion pendulums Kozyrev measured the mutual force between two masses of different materials, or the force acting on a test body if the other body is heated or cooled, or if the other body is an electric energized vacuum tube, a charging or discharging battery or simply a salt-water solution. All this (and many other) objects were able to deflect the test mass. Especially significant effects can be produced with time-varying processes (for example a blinking electronic light). It becomes really astonishing that these effects can be clearly reduced by placing an organic substance containing only right-handed molecules (as natural sugar) beside the test mass. Substances made of left-handed molecules have exactly the opposite effect.

All these experiments cannot be explained with gravity, but they are well within Kozyrev's three axioms about time. Time is an important but yet unexplored physical dimension. The left-right asymmetry and its related symmetry breaking with spin play an important role for the properties of time^[7].

According to Kozyrev the properties of time change everywhere in the universe simultaneously. No propagation of energy takes place as it's known from force fields. In all places in the universe the variation of a second happens simultaneously. Kozyrev assumed that the intensity of a time wave to a test mass falls inverse proportional to the distance of cause (for example an oscillating mass). No impulse changes (forces, accelerations) are propagating through a medium, only energy disappears at one place and appears at an other place.

A material system can be shielded against time patterns. Several solid materials as metals (especially Aluminum), glass or ceramics with a thickness of some centimeters are

sufficient. The shielding property of fluids is much lower. They need a thickness of some decimeters and gases – like Earth’s atmosphere – seems not to shield at all (or very weak). Further experiments show that only these time patterns are reflected, which increases a local time density^[18].

A shielding effect bases on the reflection of an incoming cause (wave). If we construct a box of such a shielding material, cut a slot and place a detection unit in the box, we get a device named Kozyrev camera. All we need is a telescope, where we connect the ocular to the slot of the camera. With this equipment Kozyrev was able to detect the true position of stars. Usually we only see the retarded position of stars (or the Sun), because light needs time to travel to Earth, and during this time the stars still change positions. But with a Kozyrev device the true position is clearly detectable. This is only possible if the signal of the distant star is already here (is equal to infinite propagation speed). Therefore Kozyrev didn’t use electromagnetic waves but a new kind of information which he called time pattern or time wave.

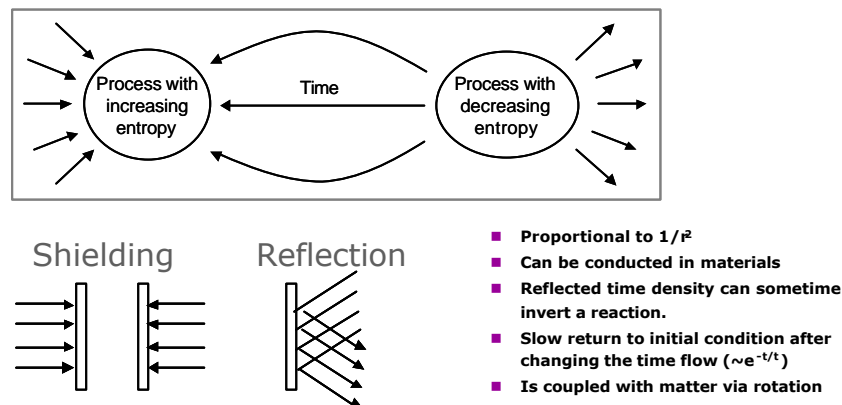


Figure 33: The global time wave as Kozyrev might have thought about it.

From all this experiments of Shnoll et. al. and Kozyrev we learn, that all processes in nature are somehow coupled together and happens absolutely synchronous. In Global Scaling theory the global background field or time wave is the cause for this time effects. This time wave (or Kozyrev’s^[17] time pattern) can be shielded, reflected and deflected. Therefore it shows similar properties as electromagnetic waves.

Experiments of Erwin Saxl

Erwin Saxl has built a sensitive torsion pendulum which is described in detail in his patent^[32]. He measured the oscillation periods very exactly with laser beams and mirrors. This gave him a very sensitive measuring device for changes in local gravity force. During the total eclipse of the Sun on March 07, 1970 he detected a significant increase in oscillation period of about 0.027%^[33]. These change is about ten times in magnitude as the gravity attraction of the moon to the torsion pendulum.

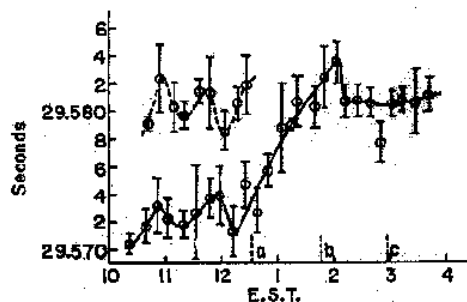


Figure 34: The oscillation period of the torsion pendulum in dependence of local time. The eclipse started at 12:31 (dotted line a), has its maximum at 13:40 (b) and ended at 14:58 (c). Two weeks later the moon was on the exact opposite and the dashed bold line has been recorded. Both curves shows a congruence in the fine spectra. (Source:

Beside such clear signals Saxl already detected 1964 that Newton's constant of gravity is not really constant but changes slightly through time. The pendulum often showed deviations or fluctuations of much higher magnitude than the resolution limit of the measuring equipment. Sometimes the same fine structure was repeated several time. For example two weeks after a total eclipse of the Sun where the moon was in exact opposite position, the same fine structure is shown in the figure above. This coincidence of **fluctuations** of an always changing measuring quantity points to a common cause.

As early as in 1964 Saxl^[31] recognized that the oscillation period of the torsion pendulum – which was placed in a Faraday cage – changes much more, if the pendulum is electric charged against Earth. Almost independently whether the voltage is positive or negative, the oscillation period increases. With a voltage of about 5000 Volt the change of signal was close to +0.3%. This effect cannot be explained with every accepted physical theory.

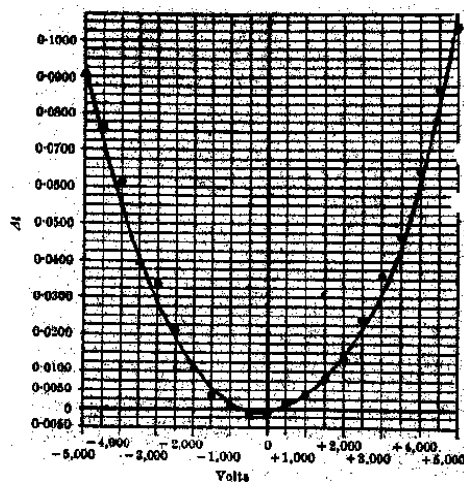


Figure 35: The oscillation period of the torsion pendulum in dependence of voltage applied against Earth. The curve is quadratic in first approximation. The delta of oscillation period Δt is set into relation to the value of about 35.2 second when no voltage is applied. (Source: Nature [31]).

Experiments of Guido Ebner and Guido Schuerch

Other impressive experiments confirming the work of Kozyrev and Saxl has been done by the chemists Guido Ebner and Heinz Schuerch in Basel (Switzerland). In charge of Ciba Geigy (now Novartis) they researched the influence of electrostatic fields to the growth and morphogenesis of living substances, if the germ, seed or eggs has been placed between two electric conducting plates carrying an electric field of 500....2000V/m for a certain time.

The outcome was very surprising for all involved parties, especially for the company itself. In the year 1989 Ciba Geigy applied for the patent „Method of enhanced fish breeding“. They describe how fishes (trouts) develop and grow much better, if their eggs have been conditioned in an electrostatic field. In comparison to standard processes, the hatch rate increased by 100...300%, the fishes became more agile and vital, they had a much higher resistance against disease and gained in weight and size up to maturity much faster.

What's not mentioned in the patent, but has been presented to the author by Guido Schuerch, was the significant change in morphogenesis. The treated fishes have a much powerful body, concise colors and a much stronger bit with elongated lower jaw. This fish form is died out since long time!

And this was only the beginning. The chemical industry was obviously not interested very much in applying and selling of this new (free of chemical) technology. Finally the two

chemists founded their own Institute of Pharmaceutical Research near Basel, where Here Guido Ebner applied for an other and very detailed patent, which was never granted. In this patent he describes the effect of electrostatic fields to several life forms (cress, wheat, corn, fern, micro-organisms, bacteria) in their early stage.

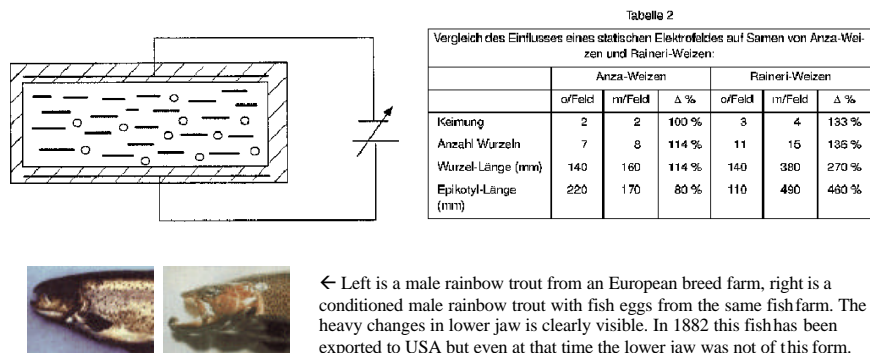


Figure 36: The method of Ebner and Schuerch: Above is a small exclusion of patent, below is a comparison in morphogenesis from rainbow trout.

Again the change in morphogenesis was highly visible. The corn grew often with more than one stalk, stalk and leaves were broader, the plant carried more and larger corncobs which are placed differently at the stalks and within 5 days they grew to three-fold cobs, which in turn again form new cobs on the top. The fern showed a completely new form of leaves already died out since millions of years. On a very special photograph Schuerch showed a fern having all sorts of leaves in one single plant. The first leaf appeared to be about 300 millions of years old where as the last grown-up leaf already looked close to today's form. And this on the very same plant! This is absolutely unbelievable for a botanist.

With the treatment by an electrostatic field – which does not have a constant efficiency at all time – living organisms are put back to a very early development stage. They often get a form which today is only known by fossils.

Chemical reactions do not take place during this treatment, because no electric current is applied to the organisms. A possible biological or physical cause for this effects are not known.

All the described experiments reveal a common – but really unexpected – point. Obviously the time pattern, or the global time wave, plays an important role. It seems to be possible to manipulate time locally to produce local an unexpected or unknown effects. This time pattern can be altered either with a change in mass density (Kozyrev) or with a change in charge density (Saxl, Ebner & Schuerch).

Time, energy and entropy

The essence in applications of Global Scaling lies in this time pattern or time wave. If we succeed to find this time pattern for a process by analyzing a huge amount of data (Shnoll), we are able to tap completely new applications. For Kozyrev the time vector and an energy flow is equivalent. *A compression in time flow of a closed system cause an increase in entropy (disorder), a decompression in time flow results in a decreasing entropy* ^[18]. Experiments compressing the time flow are accompanied by a local temperature decrease and vice-versa. Hence, Kozyrev has worked in many experiments with heating or cooling of probes.

The universe must be a thermodynamic open system to supply the standing gravity waves with energy all the time and to build up dissipative structures as atoms, matter etc.

These entropic forces are very fundamental. They are more fundamental than the known interaction forces of gravity, electrostatic or electrodynamics.

Now we take the findings of Kozyrev and apply them to a logarithmic line of arbitrary calibration. We know already that the graviton density is very high at a nodal point and in a gap the opposite is the case. We also know that only in nodes an energy exchange can take place without destroying the standing wave. This gives us the following table for the regions of a Muller fractal:

	Border areas	Nodes N ₀ , N ₂ , N ₄ , ...	Border areas	antinodes
Graviton density	increasing	high	decreasing	low
Pressure	increasing	maximum	decreasing	minimum
Entropy (disorder)	decreasing	minimum (order)	increasing	maximum (chaos)
Time flow	increasing	dense	decreasing	diluted
Thermodynamic state	optimal	open	optimal	closed
Structural state	fusion tendency	fusion or transformation	decay tendency	decay or transformation
Energy	transport	source	transport	drain

Table 1: Properties of sections in the Muller fractal

This table is valid for all even scaling layers. With odd scaling layers the two columns of the border interchange. The higher the scaling layer, the powerful are these influences. Usually our technology is not able for manipulations on the highest level, but this is probably just fine.

The monotone arrow of time is only a rough description of what really takes place in the time dimension. The homogeneity of time is an average effect. In essence time posses a fractal dimension, as other dimensions too. And similar to other values also the time traverse on the logarithmic-hyperbolic Muller fractal from the smaller values on the left to larger values on the right. Time is created with this always happening compression and decompression. Or maybe, all this is otherwise around?

Local and global time line

According to Global Scaling theory^[24] a new time line is started for each process, for each new creation, for each new living organism (Embryo genesis). The start always happens in a nodal point of both, the global and the local, process-dependent time line. So every entity has its own local time line, starting on its "birth". So Earth, the solar system, the universe but also each living thing as you and me posses its own time line.

A global time line supersedes each (lower) local time line. Hence, global events for example happening on the Sun always have an influence on local processes for example on Earth (here we speak not about electromagnetic wave or flares from the sun, but about changes in time patterns). With a smaller effect this is also the case in the other direction. These global events act simultaneously through all scaling layers down to our local processes. This is documented very well with experiments from Shnoll et. al. or Saxl. There we find daily, monthly and seasonal dependencies which document the cause of the next higher time line. And these experiments are not exceptional. An other experiment dealing with high voltage is for example the so-called Biefeld-Brown effect.

An asymmetric constructed capacitor^[4], charged with a static voltage of about 30kV or more, accelerates in direction of the positive polarity. This effect does not only base on ion wind, because according to Brown it shall work also in oil or in vacuum. Thomas Townsend Brown found beside other thing, that this accelerating force is not always constant but depends on seasonal and daily conditions.

There exists an other quite simple experiment to find influences of day, month or year periods. It's the water drop experiment first published by Nobel laureate Philippe Lenard^[19], and re-discovered from Gunnar Nörling and Olof Alexandersson^[26]. In this experiment the electric water influence on free falling, pure water is increased by copper plates on the ground. This copper plates get charged against Earth of about 10kV. This plates then can be discharged through spark gaps or neon tubes. The discharge frequency depends mainly on the amount of charges in the copper plate, as the author has observed. Interestingly this frequency is far from constant. It varies very strongly with day and night time as well as with the moon cycles. During the day the frequency in a certain experiment was about 1 Hz, and in average during the night about 10 Hz. On full moon this increased up to 25 Hz. This produces almost a continuous light! Changes of other parameters like temperature, humidity and water quality didn't show a high correlation with the discharge frequency.

Usually the influence of a global time wave to al local experiment is very small. This might be the reason why they have not been discovered yet. But probably just nobody thought about running multiple experiments in parallel at different locations as made by Shnoll et. al. and almost nobody is willing to interpret measuring results without previously "smoothing" the measurement data. But the key to identify a local time wave influence is exactly the analysis of such simultaneous **fluctuations** in most possible and different parallel experiments.

Fluctuations

The deviation of single measurement values out of a long series of measurement data without smoothing the resulting curve are called fluctuations. As an example you may look at the curve in Figure 34. Generally it's assumed that these fluctuations are of **stochastic** nature. That means, they follow a real random chance and cannot be predicted. They are responsible for the limited certainty of each measurement. A very popular name for fluctuations is **thermal noise**. Basically such fluctuations can be identified in every measurement and they can not be eliminated completely.

Only with a systematic analysis of this fluctuations Shnoll et. al. discovered the correlation of such fluctuations within certain distances in time.

On measurement of an arbitrary physical quantity these fluctuations do occur on a certain scaling layer. These fluctuations produced by cosmic processes (cosmic background field) can be found up to the highest scaling layers. These global fluctuations have a higher impact to local processes than local fluctuations. Local fluctuations are mostly limited to one single (lowest) scaling layer.

The role of thermodynamics

Fluctuations are also interpreted as measurement uncertainty. Usually this shall be eliminated by means of statistical methods. To analyze some single data sets this might in some cases be sufficient. But it's not anymore possible to find inherent time patterns when smoothing methods are applied. Also statistic (stochastic) methods are only applicable for closed systems, for systems also, which do not have an energy and in formation exchange with the outer world. But as for example concluded in „Autopoietic Systems“^[43], this is not possible in a real world. Each observable system must be open, otherwise it cannot be observed.

This implies, that open systems can deviate to statistical laws, and surely this happens in nature with a very high probability. The only "place" in the Muller fractal to exchange energy between different processes – for example between local and global processes – are

nodal points. If two nodal points of different processes fall together, immediately an exchange of energy can occur, if required by one of the two involved processes. This time interaction (or energy interaction) will leave a traces in form of fluctuations.

Let's look again at Figure 19. A system is wandering along the logarithmic line from smaller values up to larger values and therefore passes nodes on lower scaling layers all the time. The chance, that two processes meet each other at a node in lower scaling layers is much higher compared to the chance that one or even both systems meet on a higher scaling layer.

Each time a system reaches a node, the system is open from a thermodynamic point of view. That means it's able to exchange energy with an other system without time delay. As also shown in Figure 19, each system can only be open in one single scaling layer at a particular time. In all other layers, including all higher layers, the system is thermodynamically closed and not able to exchange energy on these layers.

These permanent openings and closings along the logarithmic line are the reason for creation and destruction of structures. A creation of structures without permanent local violation of the second law of thermodynamics is simply not possible.

Prognosis of stochastic processes

It is possible to make some prognosis for the development of a certain physical quantity or about the time of next important fluctuation, if the global fluctuations or time patterns – who take influence on all local systems simultaneously – are known. Some important cosmic sources to influence local fluctuations are already documented by Shnoll et. al., Saxl and others. These source are located on our cosmic vicinity, but these are not the only ones.

If we have enough measuring data of an alleged stochastic process (as for example lottery numbers) and if we know the time pattern of the relevant global fluctuations, it's theoretically possible to make a prognosis about the upcoming fluctuations of the local process and therefore shift the hit rate above the average.

Reflection of time

According to Kozyrev it's possible to reflect time waves with optimized reflecting materials as for example Aluminum. This reflection is not an inversion (backward running film) because causality is still valid for a reflected time wave. Only the vector direction of the time wave changes.

If we now place two reflectors in parallel we can produce a multiple reflection and therefore a superposition of a time waves. This is the case for a Kozyrev camera or for the conducting plates in the experiment of Ebner and Schuerch.

This time pattern is not created by masses or gravity forces only. Also the 10^{40} times stronger electric force produce similar changes in time patterns but with much more intensity. Therefore the Ebner and Schuerch experiment delivers such impressive results.

Near field action and action-at-a-distance

Gravity as well as electrostatics follow the same inverse square law for the distance. Newton's gravity as well as Coulomb's electrostatics can both be formulated with an action-at-a-distance formalism, that means, force changes are transmitted immediately without delay. This has been formulated in 1865 by Wilhelm Eduard Weber^[48] for electrostatics. In the year 1865 James Clerk Maxwell^[21] published his theory of contact action, i.e. a force acting with a finite velocity. After that Hermann Helmholtz and Heinrich Hertz debated many years about the speed of electrodynamics and electrostatic effects^[37]. Today this is almost forgotten.

Recently Andrew Chubykalo and Roman Smirnov-Rueda^[6] have found a theoretic base that electrostatics can only be correct deduced from Maxwell's equations, if we assume that its behavior is similar to an action-at-a-distance principle. Additionally the author^[45]

has shown that Ampere's formula for induction laws between two current carrying wires cannot be derived from Maxwell's equations when the retarded Liénard-Wiechert potentials are used. The principle of induction seems not in all cases to follow the classical field theory. There exists two kind of interactions, which are fundamentally different.

1. *The force between relative resting or continuous moving masses (or charges) is transmitted simultaneously according to the action-at-a-distance principle and decreases according to the proportionality $1/r^2$.*
2. *The force between relatively accelerating charges (or masses) happens with a delay according to a finite transmitting velocity and reduces according to the proportionality $1/r$.*

The simultaneous force part decreases much faster with growing distance than the delayed force part and therefore is most often not noticed in the noise of the signal. The poles for the force of action-at-a-distance can be described with scalar waves.

The weak force according to the first principle are the entropic or constructive forces (Schauberger, Russell), whereas the forces according to the second principle represent a destructive or reducing behavior. But only the interplay between this two principles enables the creation of structures as we know them.

Energy exchange via nodal points

If two nodes each of a local and a global process meet each other, an energy exchange is possible. The effects will be as higher, the higher the scaling layer of the affected nodes are. But most of the time this energy exchange takes place just once as a lightning in thunderstorm and therefore it's not usable in technical applications.

To achieve a steady energy flow an interaction between two stable node-pairs is necessary. Then energy can be drawn from one process to an other through one node-pair and feed back via the second node-pair (energy cannot be consumed, but flow). This requires a resonance condition between at least one global and one local time pattern. For a permanent energy flow such a resonance coupling is basically essential. In practice this is very difficult to obtain because the Muller fraction of the time wave is highly non-linear.

To start a resonance coupling we must first establish an oscillation process (let's call it primary process) on the local time wave (Kozyrev, Ebner & Schürch). This can be achieved with electric dipoles (Ebner-Schuerch) or with materials of high density (Kozyrev). Then it is important to know which global nodes will couple to which local nodes.

To increase the probability that two nodes of a local and of a global process fit together, we can take care that one process uses much faster oscillations than the other one. Let's look at the two most stable elementary particles, the proton and the electron. To establish their long lifetime they must be in an extremely precise resonance coupling with the global background time wave. These particles are super-stable, that means, their continuous fractions end at nodal points. Therefore they are able to exchange their electric forces very intensively (gravity, electrostatics). Then these forces decrease the local entropy (they are constructive).

According to impulse law, a force via nodal points leads to an acceleration of masses or charges. As a result these masses or charges radiates energy. Such kind of coupling to the global time wave is most likely not very efficient, because it will not be easy to re-collect the radiated energy. Therefore the radiated energy is lost as heat and causes local increase of entropy (destructive). But if this acceleration is made in a direction compatible to the primary process, it can be possible to establish a stable energy loop, whereas a load to utilize this flowing energy is an important part of this energy loop. For doing this, also a secondary circuit will be required. And between the primary and secondary circuit a storing device (as a capacitor or battery) must be placed to enable energy in- and outflow all the time.

A small hint about the type of global process we may tap for energy generation originates from Nicola Tesla.

Possible energy source: The cosmic background radiation

The spectra of the three Kelvin background radiation was first detected accidentally in 1965 by the two radio astronomers Penzias and Wilson by using a horn antenna. But already in 1934 Nicola Tesla^[40] reported a radiation from outer space with a wave length of 1 to 2 millimeters. In this article he writes, that he has measured this radiation already in 1900, i.e. 34 years before first publication: „*I may state that even waves one or two millimeters long, which I produced thirty-four years ago, provided that they carry sufficient energy, can be transmitted around the globe*“. 1900 was probably his most important year where he conducted his famous Colorado Springs experiments. Already just before his death he again talked about this radiation and said^[41]: „*The effects at great elevations are due to waves of extremely small lengths produced by the sun in a certain region of the atmosphere. This is the discovery I wish to make known*“.

The spectra of this cosmic background radiation is well known today and matches very well to a thermal radiation of a black body having 2.726 Kelvin temperature. In the standard model the cause of this radiation is the big bang. But with newer pictures from Hubble telescope the big bang thesis comes more and more under pressure. The Global Scaling theory does not require a big bang to create the structures of today's world. The only condition is a thermodynamic open universe, that's it. By the way, also the big bang is a high violation of the second law of thermodynamics, isn't it? In contrast Global Scaling explains a more or less steady growth and evolution of forms by using some basic laws.

But if – as assumed in Global Scaling – no big bang happened milliars of years ago, there must be an other explanation of the background microwave radiation in the universe. Obviously this radiation is caused by space-time itself. The distribution of this radiation does not reveal an origin (where a big bang should have happened) nor does it increase around galaxies or stars. The maximum of this background radiation is exact in a nodal point with very high priority. We are able to detect this background radiation, because electrons are influenced by it. That means, the electron is in a steady contact with this background field, or we may also conclude, the electron has some kind of resonance coupling to the background field. This makes it in principle possible tap more energy out of this background field as one might expect.

On the logarithmic frequency line with phase set to $P=1$ the background radiation has its maximum very close to the node $N_0 = -30$. The exact node gives a frequency of 133.55GHz. The reciprocal value is the node $N_0 = 30$ on the logarithmic length line and gives the wave length of 2.247mm in vacuum. The cosmic background field offers many nodal points for resonance coupling with several local processes. Once this problem is solved, a new and clean energy source will be the result.

Acknowledgement

The first thank is addressed to Dr. rer. nat. Hartmut Muller. Without his outstanding publications this paper would not exist. Also a special thank is addressed to all referenced authors. Without their previous work the drawing of a whole picture will never be possible.

Global Scaling Lectures

With this short summary you have got an overview about the Global Scaling theory only. To learn more about this theory and to learn how to use it in technical or business applications, more profound knowledge is necessary. Therefore we highly recommend the Global Scaling seminars lectured at the [Institute for Space-Energy-Research GmbH](#) (IREF) in Wolfratshausen, near Munich, Germany, www.globalscaling.de.

Important: This document serves for information only. AW-Verlag explicitly points to the fact that with the content of this document it is not possible to use the Global Scaling theory appropriate for projects of any kind. AW-Verlag rejects every claim for liability for direct or indirect damage or loss which may occur by inappropriate use of the Global Scaling theory.

Appendices

7.

Appendix 1: Continuous fractions of some irrational numbers

$$\begin{aligned} \phi &= 1.6180339 \dots = [1; 1, 1, 1, 1, 1, 1, 1, 1, 1, 1, 1, 1, 1, 1, 1, 1, 1, \dots] \\ \frac{1}{\phi} &= 0.6180339 \dots = [0; 1, 1, 1, 1, 1, 1, 1, 1, 1, 1, 1, 1, 1, 1, 1, 1, 1, \dots] = \phi - 1 \\ \phi^2 &= 2.6180339 \dots = [2; 1, 1, 1, 1, 1, 1, 1, 1, 1, 1, 1, 1, 1, 1, 1, 1, 1, \dots] = \phi + 1 \\ \sqrt{2} &= 1.4142135 \dots = [1; 2, 2, 2, 2, 2, 2, 2, 2, 2, 2, 2, 2, 2, 2, 2, 2, 2, \dots] \\ \sqrt{3} &= 1.7320508 \dots = [1; 1, 2, 1, 2, 1, 2, 1, 2, 1, 2, 1, 2, 1, 2, 1, 2, 1, \dots] \\ \sqrt{5} &= 2.2360679 \dots = [2; 4, 4, 4, 4, 4, 4, 4, 4, 4, 4, 4, 4, 4, 4, 4, 4, 4, \dots] \\ \sqrt{6} &= 2.4494897 \dots = [2; 2, 4, 2, 4, 2, 4, 2, 4, 2, 4, 2, 4, 2, 4, 2, 4, 2, \dots] \\ \sqrt{7} &= 2.6457513 \dots = [2; 1, 1, 1, 4, 1, 1, 1, 4, 1, 1, 1, 4, 1, 1, 1, 4, 1, \dots] \\ \sqrt{8} &= 2.8284271 \dots = [2; 1, 4, 1, 4, 1, 4, 1, 4, 1, 4, 1, 4, 1, 4, 1, 4, 1, \dots] \\ \sqrt{10} &= 3.1622776 \dots = [3; 6, 6, 6, 6, 6, 6, 6, 6, 6, 6, 6, 6, 6, 6, 6, 6, 6, \dots] \\ \sqrt{11} &= 3.3166247 \dots = [3; 3, 6, 3, 6, 3, 6, 3, 6, 3, 6, 3, 6, 3, 6, 3, 6, 3, \dots] \\ \sqrt{12} &= 3.4641016 \dots = [3; 2, 6, 2, 6, 2, 6, 2, 6, 2, 6, 2, 6, 2, 6, 2, 6, 2, \dots] \\ e &= 2.7182818 \dots = [2; 1, 2, 1, 1, 4, 1, 1, 6, 1, 1, 8, 1, 1, 10, 1, 1, 12, 1, 1, 14, 1, \dots] \\ &\quad \text{(Euler, 1737)} \\ e &= 2.7182818 \dots = 2 + \frac{2}{2} + \frac{3}{3} + \frac{4}{4} + \frac{5}{5} + \dots \\ e &= 2.7182818 \dots = 2 + \frac{1}{1} + \frac{1}{2} + \frac{2}{3} + \frac{3}{4} + \dots \\ \frac{e-1}{e+1} &= 0.4621171 \dots = [0; 2, 6, 10, 14, 18, 22, 26, 30, \dots] \\ e^2 &= 7.3890560 \dots = [7; 2, 1, 1, 3, 18, 5, 1, 1, 6, 30, 8, 1, 1, 9, 42, 11, 1, 1, 12, 54, 14, \dots] \\ &\quad \text{(Stieltjes, ca. 1890)} \\ \sqrt{e} &= 1.6487212 \dots = [1; 1, 1, 1, 5, 1, 1, 9, 1, 1, 13, 1, 1, 17, 1, 1, 21, 1, 1, 25, 1, 1, \dots] \\ &\quad \text{(Sundman, 1895)} \\ e^{\frac{1}{n}} &= \dots = [1; n-1, 1, 1, 3n-1, 1, 1, 5n-1, 1, 1, 7n-1, 1, 1, \dots] \\ e^{\frac{2}{2n+1}} &= \dots = [1; n, 12n+6, 5n+2, 1, 1, 7n+3, 36n+8, 11n+5, 1, \\ &\quad 1, 13n+6, 60n+30, 17n+8, 1, 1, 19n+9, 84n+42, 23n+12, \dots] \\ \pi &= 3.1415926 \dots = [3; 7, 15, 1, 292, 1, 1, 1, 2, 1, 3, 1, 14, 2, 1, 1, 2, 2, 2, 2, 1, 84, \dots] \end{aligned}$$

$$\pi = 3.1415926 \dots = 3 + \frac{1^2}{6} + \frac{3^2}{6} + \frac{5^2}{6} + \frac{7^2}{6} + \dots \quad (\text{Lange, 1999})$$

$$\frac{\pi}{2} = 1.5707563 \dots = 1 - \frac{1}{1+} \frac{1 \cdot 2}{1+} \frac{2 \cdot 3}{1+} \frac{3 \cdot 4}{1+} + \dots \quad (\text{Euler, 1739})$$

$$\frac{\pi}{2} = 1.5707563 \dots = 1 + \frac{2}{3+} \frac{1 \cdot 3}{4+} \frac{3 \cdot 5}{4+} \frac{5 \cdot 7}{4+} + \dots \quad (\text{Euler, 1783})$$

$$\frac{\pi}{2} = 1.5707563 \dots = 1 - \frac{2}{3-} \frac{2 \cdot 3}{1-} \frac{1 \cdot 2}{3-} \frac{4 \cdot 5}{1-} + \dots \quad (\text{Stern, 1833})$$

$$\frac{4}{\pi} = 1.2732395 \dots = 1 + \frac{1^2}{2+} \frac{3^2}{2+} \frac{5^2}{2+} \frac{7^2}{2+} + \dots \quad (\text{Brounker, 1658; Euler 1775})$$

$$\frac{4}{\pi} = 1.2732395 \dots = 1 + \frac{1^2}{3+} \frac{2^2}{5+} \frac{3^2}{7+} \frac{4^2}{9+} + \dots$$

$$\frac{4}{\pi} = 1.2732395 \dots = 1 + \frac{2}{7+} \frac{1 \cdot 3}{8+} \frac{3 \cdot 5}{8+} \frac{5 \cdot 7}{8+} + \dots \quad (\text{Euler 1783})$$

$$\frac{3}{4}\pi = 2.3561944 \dots = 2 + \frac{1}{2+} \frac{1 \cdot 3}{2+} \frac{2 \cdot 4}{2+} \frac{3 \cdot 5}{2+} + \dots \quad (\text{Euler, 1739})$$

$$\sqrt{\pi} = 1.7724538 \dots = [1; 1, 3, 2, 1, 1, 6, 1, 28, 13, 1, 1, 2, 18, 1, 1, 1, 83, 1, 4, \dots]$$

$$\frac{\pi^2}{6} = 1.6449340 \dots = 1 + \frac{1}{1+} \frac{1 \cdot 1}{1+} \frac{1 \cdot 2}{1+} \frac{2 \cdot 2}{1+} \frac{2 \cdot 3}{1+} \frac{3 \cdot 3}{1+} \frac{3 \cdot 4}{1+} + \dots$$

$$\frac{12}{\pi^2} = 1.2158542 \dots = 1 + \frac{1^4}{3+} \frac{2^4}{5+} \frac{3^4}{7+} \frac{4^4}{9+} + \dots$$

Appendix 2: Calibration units

To calculate the calibration units, some physical constants are required, These are^[11]:

m_p	proton rest mass	1.672 623 1	$\pm 0.000\,001\,0$	10^{-27}	[kg]
u	atomic mass unit	1.660 540 2	$\pm 0.000\,001\,0$	10^{-27}	[kg]
c	speed of light in vacuum	2.997 924 58	(exact)	10^8	[m/s]
ϵ_0	electric field constant	8.854 187 817	...	10^{-12}	[F/m]
h	Planck's constant	6.626 075 5	$\pm 0.000\,004\,0$	10^{-34}	[Js]
q	elementary charge	1.602 177 33	$\pm 0.000\,000\,49$	10^{-19}	[C]
{e}	electron volts	1.602 177 33	$\pm 0.000\,000\,49$	10^{-19}	[J]
k	Boltzmann's constant	1.380 658	$\pm 0.000\,012$	10^{-23}	[J/K]
G	gravity constant	6.672 59	$\pm 0.000\,85$	10^{-11}	[m ³ /kg s ²]

Calibration unit for [eV]

$$[eV]_p = \frac{m_p \cdot c^2}{\{e\}} = (9.382\,723\,4 \pm 0.000\,084\,8) \cdot 10^8 \text{ [eV]}, \quad (59)$$

Calibration unit for [u]

$$[u]_p = \frac{m_p}{u} = (1.007\,276\,5 \pm 0.000\,001\,2) [], \quad (60)$$

Calibration unit for [m]

$$\lambda_p = \frac{h}{2\pi \cdot c \cdot m_p} = (2.103\,089\,3 \pm 0.000\,002\,5) \cdot 10^{-16} \text{ [m]}, \quad (61)$$

Calibration unit for [Hz]

$$f_p = \frac{2\pi \cdot c^2 \cdot m_p}{h} = (1.425\,486\,1 \pm 0.000\,001\,7) \cdot 10^{24} \text{ [Hz]}, \quad (62)$$

Calibration unit for [s]

$$\tau_p = \frac{h}{2\pi \cdot c^2 \cdot m_p} = (7.015\,150\,8 \pm 0.000\,008\,4) \cdot 10^{-25} \text{ [s]}, \quad (63)$$

Calibration unit for [K]

$$T_p = \frac{m_p \cdot c^2}{k} = (1.088\,813\,2 \pm 0.000\,010\,1) \cdot 10^{13} \text{ [K]}, \quad (64)$$

Calibration unit for [°C]

$$T_p = \frac{m_p \cdot c^2}{k} - 273.15 \text{ [°C]}, \quad (65)$$

Appendix 3: Values of mass line

[kg]	Ymin: 1.672622123E-27 Ymax: 1.672624097E-27	Phase = h (1)	
-54	2.17E-51 1.61E-50	Photon, Graviton	27 3.27E-16 2.42E-15
-51	4.37E-50 3.23E-49		30 6.58E-15 4.86E-14
-48	8.77E-49 6.48E-48		33 1.32E-13 9.76E-13
-45	1.76E-47 1.30E-46		36 2.65E-12 1.96E-11
-42	3.54E-46 2.61E-45		39 5.33E-11 3.94E-10
-39	7.11E-45 5.25E-44		42 1.07E-09 7.91E-09
-36	1.43E-43 1.05E-42		45 2.15E-08 1.59E-07
-33	2.87E-42 2.12E-41		48 4.32E-07 3.19E-06
-30	5.76E-41 4.25E-40		51 8.67E-06 6.41E-05
-27	1.16E-39 8.55E-39		54 1.74E-04 1.29E-03
-24	2.32E-38 1.72E-37		57 3.50E-03 2.59E-02
-21	4.67E-37 3.45E-36		60 7.03E-02 5.19E-01
-18	9.37E-36 6.92E-35		63 1.41E+00 1.04E+01
-15	1.88E-34 1.39E-33		66 2.83E+01 2.09E+02
-12	3.78E-33 2.79E-32		69 5.69E+02 4.21E+03
-9	7.59E-32 5.61E-31		72 1.14E+04 8.45E+04
-6	1.53E-30 1.13E-29		75 2.30E+05 1.70E+06
-3	3.06E-29 2.26E-28		78 4.61E+06 3.41E+07
0	6.15E-28 4.55E-27	Proton	81 9.27E+07 6.85E+08
3	1.24E-26 9.13E-26		84 1.86E+09 1.38E+10
6	2.48E-25 1.83E-24		87 3.74E+10 2.76E+11
9	4.99E-24 3.68E-23		90 7.51E+11 5.55E+12
12	1.00E-22 7.40E-22		93 1.51E+13 1.11E+14
15	2.01E-21 1.49E-20		96 3.03E+14 2.24E+15
18	4.04E-20 2.99E-19		99 6.08E+15 4.50E+16
21	8.11E-19 6.00E-18		102 1.22E+17 9.03E+17
24	1.63E-17 1.20E-16		105 2.45E+18 1.81E+19
108	4.93E+19 3.64E+20		
111	9.90E+20 7.32E+21		
114	1.99E+22 1.47E+23	Moon	
117	4.00E+23 2.95E+24	Mars	
120	8.02E+24 5.93E+25		
123	1.61E+26 1.19E+27	Saturn	
126	3.24E+27 2.39E+28		
129	6.50E+28 4.80E+29		
132	1.31E+30 9.65E+30	Sun	
135	2.62E+31 1.94E+32		
138	5.27E+32 3.89E+33		
141	1.06E+34 7.82E+34		
144	2.13E+35 1.57E+36		
147	4.27E+36 3.15E+37		
150	8.58E+37 6.34E+38		
153	1.72E+39 1.27E+40		
156	3.46E+40 2.56E+41		
159	6.95E+41 5.13E+42		
162	1.40E+43 1.03E+44		
165	2.80E+44 2.07E+45		
168	5.63E+45 4.16E+46		
171	1.13E+47 8.36E+47		
174	2.27E+48 1.68E+49		
177	4.56E+49 3.37E+50		
180	9.16E+50 6.77E+51		
183	1.84E+52 1.36E+53		
186	3.70E+53 2.73E+54		
189	7.43E+54 5.49E+55	Universe	

Appendix 4: Table of some super-stable masses

			Ymin			
			1.672622123E-27 [kg]			
			Ymax			
			1.672624097E-27 [kg]			
			Y			
			1.672623110E-27 [kg]			
N ₀	N ₁	N ₂	<i>ln</i> (1)	<i>ln</i> (6)	<i>ln</i> (1/6)	
-36	27	9	4.28585E-43	2.57151E-42	7.14308E-44	
-36	18	18	4.50647E-43	2.70388E-42	7.51078E-44	
-36	9	27	5.23017E-43	3.13810E-42	8.71696E-44	
-27	-9	36	2.31828E-39	1.39097E-38	3.86381E-40	
-27	36	-9	3.39248E-39	2.03549E-38	5.65413E-40	
-27	18	9	3.64712E-39	2.18827E-38	6.07853E-40	
-27	9	18	4.23110E-39	2.53866E-38	7.05183E-40	
-18	-18	36	2.18895E-35	1.31337E-34	3.64825E-36	
-18	36	-18	2.74807E-35	1.64884E-34	4.58012E-36	
-18	9	9	3.41200E-35	2.04720E-34	5.68667E-36	
-9	-9	18	1.51823E-31	9.10940E-31	2.53039E-32	
-9	-18	27	1.77335E-31	1.06401E-30	2.95558E-32	
-9	18	-9	2.40687E-31	1.44412E-30	4.01145E-32	
9	-18	9	1.16237E-23	6.97421E-23	1.93728E-24	
9	18	-27	1.57762E-23	9.46572E-23	2.62937E-24	
9	9	-18	1.84271E-23	1.10563E-22	3.07119E-24	
18	-9	-9	8.19950E-20	4.91970E-19	1.36658E-20	
18	-36	18	1.01805E-19	6.10828E-19	1.69675E-20	
18	18	-36	1.27809E-19	7.66852E-19	2.13014E-20	
27	-9	-18	6.61216E-16	3.96729E-15	1.10203E-16	
27	-18	-9	7.67090E-16	4.60254E-15	1.27848E-16	
27	-36	9	8.24668E-16	4.94801E-15	1.37445E-16	
27	9	-36	1.20678E-15	7.24070E-15	2.01131E-16	
36	-9	-27	5.34909E-12	3.20945E-11	8.91515E-13	
36	-18	-18	6.20812E-12	3.72487E-11	1.03469E-12	
36	-27	-9	6.52769E-12	3.91661E-11	1.08795E-12	
54	-27	-27	4.28291E-04	2.56975E-03	7.13818E-05	
72	-36	-36	2.88321E+04	1.72993E+05	4.80536E+03	
90	-45	-45	1.92177E+12	1.15306E+13	3.20296E+11	
108	-54	-54	1.27456E+20	7.64737E+20	2.12427E+19	
126	-63	-63	8.42902E+27	5.05741E+28	1.40484E+27	
144	-72	-72	5.56437E+35	3.33862E+36	9.27394E+34	
160	-80	-80	4.96323E+42	2.97794E+43	8.27206E+41	

Appendix 5: Values of length line

[m]	Ymin: 2.103086790E-16 Ymax: 2.103091818E-16	Phase = h (1)	
-54	2.73E-40 2.02E-39	Photon, Graviton	27 4.12E-05 3.04E-04
-51	5.49E-39 4.06E-38		30 8.27E-04 6.11E-03
-48	1.10E-37 8.15E-37		33 1.66E-02 1.23E-01
-45	2.21E-36 1.64E-35		36 3.34E-01 2.46E+00
-42	4.45E-35 3.29E-34		39 6.70E+00 4.95E+01
-39	8.93E-34 6.60E-33		42 1.35E+02 9.94E+02
-36	1.79E-32 1.33E-31		45 2.70E+03 2.00E+04
-33	3.60E-31 2.66E-30		48 5.43E+04 4.01E+05
-30	7.24E-30 5.35E-29		51 1.09E+06 8.06E+06
-27	1.45E-28 1.07E-27		54 2.19E+07 1.62E+08
-24	2.92E-27 2.16E-26		57 4.40E+08 3.25E+09
-21	5.87E-26 4.33E-25		60 8.84E+09 6.53E+10
-18	1.18E-24 8.71E-24	Neutrino	63 1.77E+11 1.31E+12
-15	2.37E-23 1.75E-22		66 3.56E+12 2.63E+13
-12	4.75E-22 3.51E-21	Particle nucleus	69 7.16E+13 5.29E+14
-9	9.55E-21 7.06E-20	Electron	72 1.44E+15 1.06E+16
-6	1.92E-19 1.42E-18	Elementary particles	75 2.89E+16 2.13E+17
-3	3.85E-18 2.85E-17		78 5.80E+17 4.29E+18
0	7.74E-17 5.72E-16	Proton	81 1.17E+19 8.61E+19
3	1.55E-15 1.15E-14		84 2.34E+20 1.73E+21
6	3.12E-14 2.31E-13	Atomic nucleus	87 4.70E+21 3.47E+22
9	6.27E-13 4.63E-12		90 9.44E+22 6.98E+23
12	1.26E-11 9.30E-11		93 1.90E+24 1.40E+25
15	2.53E-10 1.87E-09	Atoms	96 3.81E+25 2.81E+26
18	5.08E-09 3.75E-08		99 7.65E+26 5.65E+27
21	1.02E-07 7.54E-07		102 1.54E+28 1.14E+29
24	2.05E-06 1.51E-05	Cell nucleus	105 3.09E+29 2.28E+30

108-

6.20E+30
4.58E+31

 Universe

Appendix 6: Values of frequency line

[Hz]	Ymin: 1.425484401E+24 Ymax: 1.425487809E+24	Phase = ln(1)	54- 1.48E+47 1.10E+48	
-108	6.54E-24 4.84E-23	-27	9.86E+11 7.28E+12	
-105	1.31E-22 9.71E-22	-24	1.98E+13 1.46E+14	
-102	2.64E-21 1.95E-20	-21	3.98E+14 2.94E+15	visible light UV-A,B
-99	5.30E-20 3.92E-19	-18	7.99E+15 5.90E+16	UV-C
-96	1.07E-18 7.87E-18	-15	1.60E+17 1.19E+18	radiation
-93	2.14E-17 1.58E-16	-12	3.22E+18 2.38E+19	
-90	4.30E-16 3.18E-15	-9	6.47E+19 4.78E+20	Gamma- radiation
-87	8.63E-15 6.38E-14	-6	1.30E+21 9.60E+21	
-84	1.73E-13 1.28E-12	-3	2.61E+22 1.93E+23	
-81	3.48E-12 2.57E-11	0	5.24E+23 3.87E+24	
-78	6.99E-11 5.17E-10	3	1.05E+25 7.78E+25	Cosmic radiation
-75	1.40E-09 1.04E-08	6	2.12E+26 1.56E+27	
-72	2.82E-08 2.08E-07	9	4.25E+27 3.14E+28	
-69	5.67E-07 4.19E-06	12	8.53E+28 6.31E+29	
-66	1.14E-05 8.41E-05	15	1.71E+30 1.27E+31	
-63	2.29E-04 1.69E-03	18	3.44E+31 2.54E+32	
-60	4.59E-03 3.39E-02	21	6.92E+32 5.11E+33	
-57	9.22E-02 6.82E-01	24	1.39E+34 1.03E+35	
-54	1.85E+00 1.37E+01	27	2.79E+35 2.06E+36	
-51	3.72E+01 2.75E+02	30	5.60E+36 4.14E+37	
-48	7.47E+02 5.52E+03	33	1.13E+38 8.32E+38	
-45	1.50E+04 1.11E+05	36	2.26E+39 1.67E+40	
-42	3.02E+05 2.23E+06	39	4.54E+40 3.36E+41	
-39	6.06E+06 4.47E+07	42	9.12E+41 6.74E+42	
-36	1.22E+08 8.99E+08	45	1.83E+43 1.35E+44	
-33	2.44E+09 1.81E+10	48	3.68E+44 2.72E+45	
-30	4.91E+10 3.63E+11	51	7.39E+45 5.46E+46	

Figures

Figure 1: Cislenco [7]: The distribution of species regarding organism mass plotted on a logarithmic scale. The regular distance between the maximums are clear visible.	5
Figure 2: The Gauss'ian regular distribution is expected for additive growth processes whereas the logarithmic distribution arises for multiplicative (natural) growth processes [12]......	6
Figure 3: The grid stands for the energetic ground state of space. Spontaneous emission and absorption of particles and anti-particles take place within a very short time. The existence of the particles cannot be proven directly but indirectly via the effects of the resulting zero-point radiation.	7
Figure 4: The Experiment of von Grunberg and Bechinger: The „larger“ polystyrene balls in a water solution are pressed together by the „smaller“ polystyrene balls.....	7
Figure 5: The three basic attractors for a growth function: static – oscillating - chaotic.	9
Figure 6: A beads with 1, 2, 3, ..., N beads of same mass have a corresponding number of possible transversal resonance frequencies.....	10
Figure 7: The general oscillating beads.....	11
Figure 8: Regular distance of 3 of N_0 on the logarithmic line.	19
Figure 9: Hyperbolic distances because of $N_i/3$ on the logarithmic line.....	19
Figure 10: The linear chopping of the logarithmic line in the partial areas $N_i \pm 1$	19
Figure 11: Hyperbolic chopping within the partial areas $N_i \pm 1$	20
Figure 12: Regular and hyperbolic chopping of logarithmic line.....	20
Figure 13: The structure of the Muller fractal on a logarithmic line.....	22
Figure 14: The structure of a Cantor fractal on a linear line.....	22
Figure 15: The influence of different numerators to the Muller fractal.	24
Figure 16: The graphic interaction with the Muller fractal with the software GSC 3000 Enterprise.....	24
Figure 17: The experiment of August Kundt.....	25
Figure 18: The effect of a superposition of several standing waves on a beads with freely moveable beads.....	26
Figure 19: The traveling on the mass line.....	27
Figure 20: Qualitative information about the different sections within a Muller fractal.....	28
Figure 21: The projection of the Muller fractal from a logarithmic line to a linear line.	29
Figure 22: The two Muller fractals shifted by 90° against each other. This shift corresponds to 1.5 logarithmic units on the logarithmic line.....	29
Figure 23: Phase shift on a logarithmic line.....	30
Figure 24: The four oscillation modes of the G-wave.....	32
Figure 25: Some cosmic structure relations.....	33
Figure 26: The electromagnetic spectra in the range of visible light.....	34
Figure 27: The gradient of graviton velocity (green line) in a small section of the Muller fractal.	35
Figure 28: Two histogram analysis results made by Professor Simon Shnoll (Source: Physics - Uspekhi and Physics and Chemistry of the Earth).....	36
Figure 29: A sequence of 12 consecutive histograms (Source: Physics-Uspekhi).....	37
Figure 30: Sorting of most similar histogram-pairs (Source: Physics Uspekhi).....	37
Figure 31: Distribution of time intervals between most similar-shaped histogram-pairs (Source: Physics Uspekhi).....	38
Figure 32: Synchronicity of simultaneous measurement of α -decay of ^{239}Pu in Pushchino (Moscow) and of β -decay of ^{137}Cs in Dubna. Shown are the number of pairs N of similar histograms and the corresponding time of occurrence in minutes. The most probable situation describes the simultaneous appearance of similar histograms from both different physical processes. (Source: Physics Uspekhi).....	39
Figure 33: The global time wave as Kozyrev might have thought about it.....	41

Figure 34: The oscillation period of the torsion pendulum in dependence of local time. The eclipse started at 12:31 (dotted line a), has its maximum at 13:40 (b) and ended at 14:58 (c). Two weeks later the moon was on the exact opposite and the dashed bold line has been recorded. Both curves show a congruence in the fine spectra. (Source: Physical Review D [33]).41

Figure 35: The oscillation period of the torsion pendulum in dependence of voltage applied against Earth. The curve is quadratic in first approximation. The delta of oscillation period Δt is set into relation to the value of about 35.2 second when no voltage is applied. (Source: Nature [31]).42

Figure 36: The method of Ebner and Schuerch: Above is a small exclusion of patent, below is a comparison in morphogenesis from rainbow trout.....43

References

- [1] D'ALEMBERT Jean le Rond, „Recherches sur la courbe que forme une corde tendue mise en vibration“, *Mem. de l'Acad. Sci. Berlin* **3** (1747) 214-219
- [2] BECKINGER C, D. RUDHARDT, P. LEIDERER, R. ROTH und S. DIETRICH, „Understanding Depletion Forces beyond Entropy“, *Physical Review Letters* **83** /19 (08 November 1999) 3960-3963
- [3] BEUTELSPACHER A. und B. PETRI, „Der Goldene Schnitt“, *Spektrum Verlag*
- [4] BROWN Thomas Townsend, „Electrokinetic Apparatus“, *US Patent 2'949'550* (16 August 1960)
- [5] CANTOR Georg, „Über unendliche, lineare Punktmannigfaltigkeiten“, *Mathematische Annalen* (1883)
- [6] CHUBYKALO A. E. and R. SMIRNOV-RUEDA, „Action at a distance as a full-value solution of Maxwell equations: The basis and application of the separated-potentials method“, *Physical Review E* **53** /5 (May 1996) 5373-5381; Erratum: *Physical Review E* **55** (1997) 3793
- [7] CISLENKO L. L., „Die Struktur der Fauna und Flora im Zusammenhang mit den Körpergrößen der Organismen“, (1980) *Verlag der Lomonosov-Universität, Moskau*; www.raum-energie-forschung.de/ (in Russisch)
- [8] DVOEGLAZOV Valeri V., „Significance of the Spinorial Basis in Relativistic Quantum Mechanics“, *FIZIKA B* **6** /3 (1997) 111-122
- [9] EULER Leonhard, „Sur la vibration des cordes“, *Mem. de l'Acad. Sci. Berlin* **4** (1748) 69-85
- [10] EULER Leonhard, „Introductio in analysin infinitorum“, (1748) 303
- [11] GANTMACHER F. R. und M. G. KREIN, „Oszillationsmatrizen, Oszillationskerne und kleine Schwingungen mechanischer Systeme“, *Akademie Verlag Berlin* (1960) 322-354
- [12] GEBELEIN Hans & Hans J. HEITE, „Über die Unsymmetrie biologischer Häufigkeitsverteilungen“, *Klinische Wochenschrift* **28** 3/4 (15. Januar 1950) 41-45
- [13] GRÜNBERG Hans Henning und Clemens BECHINGER, „Die Attraktivität der Unordnung“, *Spektrum der Wissenschaft* (Juni 2000) 16
- [14] GRÜNBERG Hans Henning und Clemens BECHINGER, „Entropische Kräfte“, *Physikalische Blätter* **55** (1999) 53-56
- [15] HEIM Burkhard, „Vorschlag eines Weges zur einheitlichen Beschreibung der Elementarteilchen“, *Zeitschrift für Naturforschung* **32a** (1977) 233 – 243
- [16] KHINTCHINE A., „Kettenbrüche“, *Teubner Verlagsgesellschaft, Leipzig* (1956), Moskau (1949)
- [17] KOZYREV Nikolay Alexandrovich, „Possibility of Experimental Study of Properties of Time“, (September 1967); *Time in Science and Philosophy, Prague* (1971) 111-132; reprint auf www.aw-verlag.ch
- [18] LAVRENT'EV Mikhail M and Irina A. EGANOVA, „Kozyrev's Method of Astronomical Observations: Information from true Positions of Stars, Stellar Systems, and Planets“, *Instantaneous Action at a Distance in Modern Physics – Pro and Contra, Nova Science Publishers, New York* (1999)
- [19] LENARD Philipp, „Über die Elektrizität der Wasserfälle“, *Annalen der Physik* **46** (1892) 584-636
- [20] LIDE David R, „Handbook of Chemistry and Physics“, CRC Press, 71st edition (1990)
- [21] MAXWELL James Clerk, „A Dynamical Theory of the Electromagnetic Field“, *Royal Society Transactions* **155** (1865) 459–512
- [22] MÜLLER Hartmut, „Die Skaleninvarianz physikalischer Größen stabiler Systeme als globales Evolutionsgesetz“, *Biophysikalischer Allunionskongress, Band 2, Pushzino bei Moskau* (1982)
- [23] MÜLLER Hartmut, „Global Scaling – Die Quelle der Raumenergie ist erforscht“, *raum&zeit* **106** (Juni 2000) 34-50
- [24] MÜLLER Hartmut, „Global Scaling – Die globale Zeitwelle“, *raum&zeit* **107** (August 2000) 48-59

- [25] MÜLLER Hartmut, „Die Energiequelle des Universums“, *raum&zeit* **107** (August 2000) 68-71
- [26] NORLING Ieknolog Gunnar und Olof **Alexandersson**, „Der erweiterte Wasserfadenversuch“, *Implosion* **6** (1962) 32-37
- [27] PERRON Oskar, „Die Lehre von den Kettenbrüchen, Band 1 und 2“, Teubner Verlag, Stuttgart (1954, 1957)
- [28] PUTHOFF Harold E., „Gravity as a Zero-Point -Fluctuation Force“, *Physical Review A* **39** No.5 (01 March 1989) 2333-2342
- [29] RAFELSKI Johann, MÜLLER Berndt, „Die Struktur des Vakuums - Ein Dialog über das Nichts“, *Verlag Harri Deutsch* ISBN 3-87144-888-5 (1985)
- [30] RUSSELL Walter, „The Universal One“, *University of Science and Philosophy Press, Shenandoah* (1926)
- [31] SAXL Erwin J., „An Electrically Charged Torque Pendulum“, *Nature* (11 July 1964) 136-138
- [32] SAXL Erwin J., „Device and Method for Measuring Gravitational and Other Forces“, *US Patent* **3,357,253** (12 December 1967)
- [33] SAXL Erwin J., and Mildred ALLEN, „1970 Solar Eclipse as “Seen” by a Torsion Pendulum“, *Physical Review D* **3** No.4 (15 February 1971) 823-825
- [34] SCHAUBERGER Viktor, Verschiedene Werke veröffentlicht in *Biotechnische Schriftenreihe „Implosion“*, *Dortmund* (1933-1945)
- [35] SHNOLL S. E., V.A. KOLOMBET, E.V. POZHARSKII, T.A. ZENCHENKO, I.M. ZEREVA und A.A. KONRADOV, „Realization of discrete states during fluctuations in macroscopic processes“, *Physics Uspekhi* **41** /10 (1998) 1025-1035
- [36] SHNOLL S. E., V.A. KOLOMBET, E.V. POZHARSKII, T.A. ZENCHENKO, I.M. ZEREVA und A.A. KONRADOV, „Realization of discrete states during fluctuations in macroscopic processes“, *Physics Uspekhi* **43** /2 (2000) 205-209
- [37] SMIRNOV-RUEDA Roman, „Where Hertz’s ‘crucial’ experiments on propagation of electromagnetic interactions conclusive?“, *Instantaneous Actioon at a Distance in Modern Physics – Pro and Contra*, *Nova Science Publishers, New York* (1999) 57-73
- [38] STEEB W.-H. und A. KUNICK, „Chaos in dynamischen Systemen“, *B. I. Wissenschaftsverlag, Mannheim* (1989)
- [39] STIELTJES T. J., „Recherches sur les fractions continues“, *Annales de Fac. Sci. Toulouse* **8** (1894) 1-122; **9** (1895) 1-47
- [40] TESLA Nicola, „Radio Power will Revolutionize the World“, *Modern Mechanics and Inventions* (July 1934)
- [41] TESLA Nicola, „In the Realm of Science: Tesla. Who Predicted Radio, Now Looks Forward to Sending Waves to the Moon“, by John J. O’NEILL for *New York Herald Tribune* (22 August 1937)
- [42] THOMSON William, Sir (Lord KELVIN), „On Vortex Atoms“, *Proceedings of Royal Society of Edinburgh* **6** (1867) 94-105 / *Philosophical Magazine* **34** (1867) 15-24
- [43] WASER André, „Autopoietische Systeme und die reduktionistische Physik“, *SAFE-News* **6** (Dezember 1992) 10-27; Reprint auf Internet unter www.aw-verlag.ch
- [44] WASER André, „Der Äther in der Naturwissenschaft“, www.aw-verlag.ch
- [45] WASER André, „Zur Elektrodynamik gleichförmig bewegter Ladungen“, (2000) www.aw-verlag.ch
- [46] WASER André, „Die logarithmische Verteilung in der Natur“, *raum&zeit* **123** (Mai/Juni 2003) 35-40, www.global-scaling.ch
- [47] WASER André, „Gravitation - Das letzte Geheimnis der Physik“, *raum&zeit* **127** (Januar/Februar) 2004, www.global-scaling.ch
- [48] WEBER Wilhelm Eduard, „Elektrodynamische Maassbestimmungen“, *Abhandlungen der mathematisch-physikalischen Classe der Königlich Sächsischen Gesellschaft der Wissenschaften zu Leipzig* (1846)
- [49] WHEELER Gerald F., „The vibrating string controversy“, *American Journal of Physics* **55** /1 (January 1987) 33-37

Original publications about Global Scaling in **raum&zeit** journal

1. MULLER Hartmut, „Free Energy - Global Scaling“, *raum&zeit* Special 1, *Ehlers-Verlag GmbH*, ISBN 3-934-196-17-9; www.raum-und-zeit.de
2. MULLER Hartmut, „Gravity is an all-pervading medium“, *raum&zeit* **104** (March/April 2000) 34-39
3. MULLER Hartmut, „Gravity signals detected from space“, *raum&zeit* **104** (March/April 2000) 81-84
4. MULLER Hartmut, „Atomic fusion and super-fluidity at room temperature“, *raum&zeit* **105** (Mai/June 2000) 5-10
5. MULLER Hartmut, „Faster than light“, *raum&zeit* **105** (May/June 2000) 49-51
6. MULLER Hartmut, „Global Scaling – The source of space energy is found“, *raum&zeit* **106** (July/August 2000) 34-50
7. MULLER Hartmut, „The hot story about cold fusion“, *raum&zeit* **106** (July/August 2000) 81-84
8. MULLER Hartmut, „The global time wave“, *raum&zeit* **107** (September/October 2000) 48-59
9. MULLER Hartmut, „The energy source of universe“, *raum&zeit* **107** (September/October 2000) 68-71
10. MULLER Hartmut, „Places of rods – The secret of the pyramids is Global Scaling“, *raum&zeit* **107** (September/October 2000) 85-89
11. MULLER Hartmut, „Endotherms, cosmic coldness, sun blaze and water II“, *raum&zeit* **108** (November/December 2000) 75-79
12. MULLER Hartmut, „DNA does not contain genetic information!“, *raum&zeit* **109** (January/February 2001) 55-58
13. MULLER Hartmut, „Global Scaling before 24'000 years – As in Paris nobody hunted the mammoth“, *raum&zeit* **110** (March/April 2001) 84-89
14. MULLER Hartmut, „Why birds and reptiles live longer than mammals?“, *raum&zeit* **111** (May/June 2001) 32-38
15. MULLER Hartmut, „Die trinary logic of the universe“, *raum&zeit* **111** (May/June 2001) 54-60
16. MULLER Hartmut, „Prediction of correct lottery numbers possible“, *raum&zeit* **111** (May/June 2001) 67-69
17. WASER Andre, „The Global Scaling Calculator (GSC)“, *raum&zeit* **112** (July/August 2001) 83-86
18. MULLER Hartmut, „The Curator: GS-Infrared accelerates healing process“, *raum&zeit* **113** (September/October 2001) 32-35
19. MULLER Hartmut, „Telecommunications without electromagnetic pollution“, *raum&zeit* **114** (November/December 2001) 99-108
20. MULLER Hartmut, „Who produces the first biologic cellular phone?“, *raum&zeit* **115** (January/February 2002) 65-72
21. EHLERS Hans-Joachim, „Worldwide first public demonstration of telecommunications without electric smog“, *raum&zeit* **115** (January/February 2002) 99-102
22. PRUMBACH Siegfried, „Global energy structures of a new geomantic method widely confirmed by Global Scaling“, *raum&zeit* **116** (March/April 2002) 70-76
23. MULLER Hartmut, „With 66 Milliwatt to Australia“, *raum&zeit* **116** (March/April 2002) 99-105
24. MULLER Hartmut, „A sound wave created the universe“, *raum&zeit* **117** (May/June 2002) 81-92

25. MULLER Hartmut, „The universe on the number line“, *raum&zeit* **118** (July/August 2002) 79-83
26. MULLER Hartmut, „The healing effect of red light“, *raum&zeit* **119** (September/October 2002) 5
27. MULLER Hartmut, „The super-luminous grid“, *raum&zeit* **120** (November/December 2002) 28-37
28. MULLER Hartmut, „The last mystery in Egyptology“, *raum&zeit* **120** (November/December 2002) 104-106
29. MULLER Hartmut, „[Can electromagnetic pollution be avoided?](#)“, *raum&zeit* **121** (January/February 2003) 12-18
30. MULLER Hartmut, „The clock of Chronos“, *raum&zeit* **121** (January/February 2003) 66-72
31. MULLER Hartmut, „Can lottery numbers be predicted?“, *raum&zeit* **121** (January/February 2003) 84-85
32. MULLER Hartmut, „God does not play dice, he plays chess“, *raum&zeit* **122** (March/April 2003) 28-36
33. BUHLER Urs, „Therapies in harmony with the universe“, *raum&zeit* **122** (March/April 2003) 72-74
34. MULLER Hartmut, „Hope for atomic waste disposal“, *raum&zeit* **123** (May/June 2003) 19-22
35. WASER Andre, „The logarithmic distribution in nature“, *raum&zeit* **123** (May/June 2003) 35-40
36. MULLER Hartmut, „New findings in electric smog research“, *raum&zeit* **123** (May/June 2003) 83
37. OBST Arne, „Wuerth-Machine uses G-Wave“, *raum&zeit* **124** (July/August 2003) 20-23
38. KÖHLMANN Michael, „[Cosmic cycles of Maya calendar](#)“, *raum&zeit* **126** (November/December) 2003
39. MULLER Hartmut, „[The cosmos as a provider - Premiere: Wireless data transmission via cosmic background field](#)“, *raum&zeit* **127** (January/February) 2004
40. WASER Andre, „[Gravitation – The last secret in physics](#)“, *raum&zeit* **127** (January/February) 2004
41. WASER Andre, „[New: The Global Scaling Calculator 3000 Enterprise](#)“, *raum&zeit* **127** (January/February) 2004